Chapter One

A Molecular Meccano Kit

"The whole is more than the sum of the parts" – Aristotle

This **Chapter** is based on the following Review article:

Cantrill, S. J.; Pease A. R.; Stoddart, J. F. *J. Chem. Soc., Dalton Trans.* **2000**, 3715–3734.

Table of Contents

Abstract: A range of secondary dialkylammonium ($R_2NH_2^+$) ions have been shown to thread through the cavities of appropriately-sized crown ether compounds to afford interwoven complexes. X-Ray crystallographic investigations to probe the solid-state properties of these supermolecules have revealed that many subtle factors—*e.g.*, solvents of crystallization, crown ether conformations and anion interactions—can influence the nature of the overall three-dimensional superstructures. Nonetheless, a family of building blocks—namely $R_2NH_2^+$ ions and crown ethers—can be generated, which constitute a molecular meccano kit. By mixing and matching these modules in different ways, intricate interwoven supramolecular architectures can be constructed. From relatively simple beginnings—where *one* $R_2NH_2^+$ ion is threaded through *one* monotopic crown ether (DB24C8)—the designed evolution of the building blocks in the molecular meccano kit has led to more elaborate *multiply encircled* and/or *multiply threaded* superstructures. The effects of crown ether constitution, macroring size, and both crown ether as well as $R_2NH_2^+$ ion substitution, upon the solid-state behavior of these interwoven complexes have also been examined.

1.1. Introduction

One of the goals of contemporary chemistry is the construction of larger and larger 'structures'. In the realm of covalent chemistry, these 'structures' are the numerous synthetic targets—many of them complex natural products—now being pursued in laboratories around the world.[1] With a remarkable degree of precision, chemists routinely string together collections of atoms in a targeted fashion by utilizing elegant methodologies[2] which have evolved, for the most part, over the last 50 years.

From auspicious beginnings; strychnine[3] (1954) and prostaglandin $F_{2\alpha}$[4] (1969)—to name but two examples—modern organic synthesis has flourished, rising to, and indeed overcoming, such formidable challenges as palytoxin[5] (1994), taxol[6] (1994), and brevetoxin B[7] (1995). However, these triumphs have come at a considerable price. Even when they are performed in a convergent manner, these daunting syntheses are not only

time-consuming, but are also costly and inefficient in terms of materials consumed and personnel employed. The limits of traditional covalent bond-forming chemistry must also be questioned – just how far can *molecular* synthesis[8] be taken? Although there is no definitive answer to this question, as the demand for larger and larger 'structures' grows, the practicalities of utilizing the *covalent* bond—to act as the 'glue' that holds the pieces together—are debatable. This realization has prompted investigations into alternative strategies for the construction of extended 'structures' and has lead to consideration of the chemistry of the *noncovalent* bond and, consequently, interactions between molecules—*i.e.*, supramolecular chemistry[9]—and, hence, *supramolecular* synthesis.[10]

A thorough knowledge and understanding of molecular recognition processes —particularly those based upon hydrogen bonding,[11] metal-ligand coordination,[12] π–π interactions (face-to-face[13] and edge-to-face[14]), hydrophobic,[15] ion pairing[16] and van der Waals[17] interactions—facilitates the rational design of small, relatively simple building blocks—a molecular meccano kit—that are capable of assembling into larger superstructures. In effect, as a consequence of the synthetic chemist's own judicious design, the components do all of the hard work by themselves, self-assembling[18] into extended arrays by virtue of complementary recognition features.

Application of the chemistry of the noncovalent bond to the challenge of fabricating larger and larger 'structures', has proved to be very effective, resulting in the creation of many elaborate, and indeed intricate, supramolecular architectures,[10-19] as well as assisting in the realization of novel molecular topologies[20,21] held together by mechanical bonds.

When translated into the solid state, this rational design approach is the driving force behind the field of *crystal engineering*[22] – a discipline that tempts us with the prospect of, one day, being able to predict crystal structures, simply by extrapolation from the individual building blocks. However, will this day ever arrive? Whether it does or not, as time passes our understanding of the solid state can only increase, and further exploration in this arena is the only sensible way forward. Investigations in this field are exemplified by focusing on an extremely reliable supramolecular synthon, developed[23] over the past five years in the Stoddart laboratories. Although, for many years, it was known[24] that crown ethers were effective hosts for primary alkylammonium ion (RNH_3^+) guests, in recent times secondary dialkylammonium ions ($R_2NH_2^+$) also have attracted considerable interest.[25,26] The discovery that appropriately-sized crown ethers can bind $R_2NH_2^+$ ions in a *threaded*,[27] rather than a *face-to-face*,[28] manner revealed a new paradigm for the construction of extended interwoven supramolecular arrays. This Chapter will describe a journey through this particular noncovalent landscape, highlighting how each success was built upon by applying the insight gained at each stage to the incremental development of this story so far.

1.2. In the Beginning

The concept of threading a molecule, containing an NH_2^+ center, through the cavity of the crown ether dibenzo[24]crown-8 (DB24C8) was first recorded in the literature by Busch[29] in 1995, in a Communication describing a rotaxane assembled using this type of recognition motif. Independently of the Kansas group, and as an extension to their

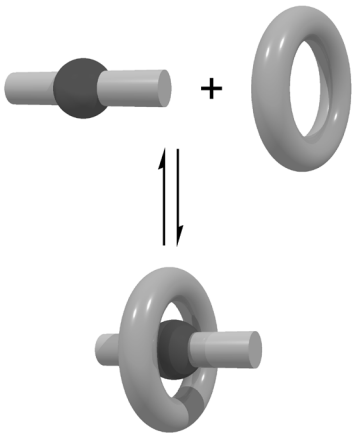

Figure 1.1. A schematic representation depicting the formation of a threaded 1:1 complex (a [2]pseudorotaxane) between two complementary species wherein the cavity of a suitably-sized macrocycle is pierced by a linear thread.

work[21] on intertwined and interlocked systems, the Stoddart group was also pursuing investigations on the potential for $R_2NH_2^+$ ions to thread (Figure 1.1) through the cavity of DB24C8 in order to generate [2]pseudorotaxanes.[30]

It was demonstrated that, in solution, the hexafluorophosphate (PF_6^-) salts of $R_2NH_2^+$ ions—such as the dibenzylammonium ion (DBA^+)—can indeed pierce the macroring of DB24C8, leading to the formation of these threaded complexes. Furthermore, the strength of the interaction was shown to depend markedly upon the nature of the solvent in which the two components were mixed. Polar solvents—*e.g.*, DMSO and DMF—are able to compete effectively with the crown ether in terms of their hydrogen bonding ability, and no complexation—*i.e.*, threading—could be observed by ^1H NMR spectroscopy. However, in poorer donor solvents—*e.g.*, Me_2CO, MeCN, and $CHCl_3$—the magnitude of the stability constant, associated with threading of the $R_2NH_2^+$ ion through the cavity of DB24C8, was shown to increase (up to values in the region of 3×10^4 M^{-1}) as the solvent polarity—as determined by the Gutmann[31] donor number—decreased. This trend suggested that the primary driving force responsible for the threading interaction is the potential for strong hydrogen bonds to be formed between the acidic NH_2^+ protons and the ring of oxygen atoms located in the DB24C8 framework.

X-Ray crystallographic analysis of single crystals obtained from a solution containing equimolar quantities of DB24C8 and DBA·PF_6 revealed[27,30] (Figure 1.2) the formation—in the solid state—of the expected 1:1 complex, possessing a pseudo-rotaxane geometry. Two crystallographically independent 1:1 complexes were present in the asymmetric unit—only one of which is shown in Figure 1.2—and, in each case, close contacts were observed between *both* of the NH_2^+ protons of the DBA^+ ion and oxygen atoms located in the polyether's macroring, indicating the formation of N^+–H···O hydrogen bonds. Additionally, in each independent complex, one of the CH_2 protons of the DBA^+ ion also approaches—within hydrogen bonding distance—one of the oxygen atoms of the DB24C8 macrocycle, further suggesting the formation of C–H···O hydrogen bonds. Therefore, the prevalence of hydrogen bonding interactions in the solid state seems to be consistent with the solution phase observations. In terms of an extended 'structure', the X-ray crystallographic analysis also revealed that individual [2]pseudorotaxane supermolecules form a column-like

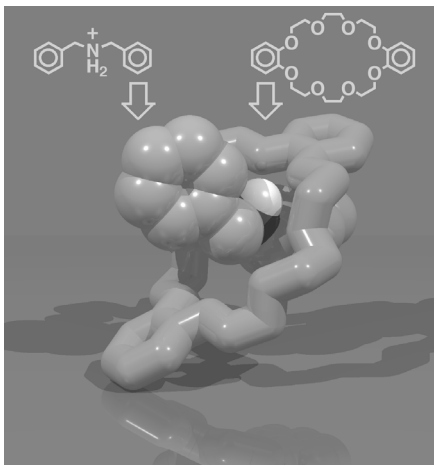

Figure 1.2. One of the two distinct superstructures adopted in the solid state by the [2]pseudorotaxane [DB24C8·DBA]$^+$.

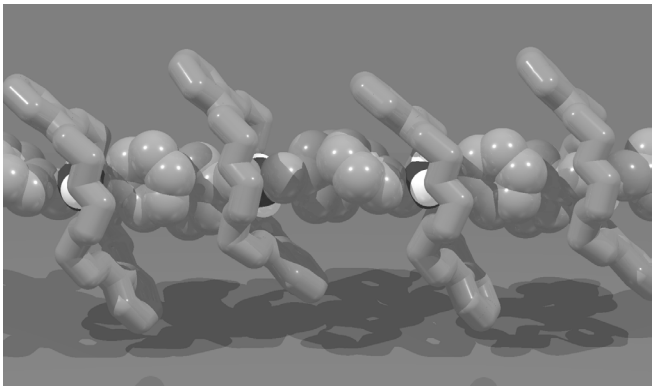

Figure 1.3. Aromatic π–π stacking of the benzyl rings of the [2]pseudorotaxane [DB24C8·DBA]$^+$ produces an infinite linear pseudopolyrotaxane.

superstructure (Figure 1.3) in which the DB24C8 macrocycles form channels through which a continuous π–π stacked chain of DBA^+ ions are threaded.

So, as 1995 drew to a close, although this molecular meccano kit was still quite small, a fundamental understanding of how and why certain building blocks associated with each other was in place. Logically, the next challenge was to increase the size of the tool-kit—in a designed, incremental fashion—by synthesizing other small building blocks that would ultimately generate an expanded repertory of self-assembled superstructures.

1.3. Multiply Encircled Complexes

Initial investigations had revealed that *one* DB24C8 macrocycle would encircle *one* DBA^+ ion. Therefore, it seemed that an obvious extension of this concept would be to make linear thread-like molecules containing more than one NH_2^+ site and explore the possibility of threading the appropriate number of DB24C8 rings onto such a species: *i.e.*, could *n* DB24C8 rings thread onto a linear molecule with *n* NH_2^+ sites, affording an [*n*+1]pseudorotaxane? To this end, thread-like molecules containing two (**1**·2PF_6), three (**2**·3PF_6), and four (**3**·4PF_6) NH_2^+ sites, respectively (Chart 1.1), were synthesized. The *molecular* synthesis complete, *supramolecular* synthesis afforded[30,32,33] the

Compound	Structure
1·2PF_6	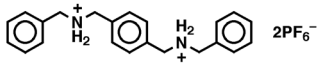
2·3PF_6	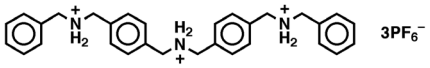
3·4PF_6	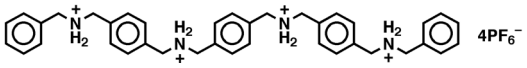

Chart 1.1

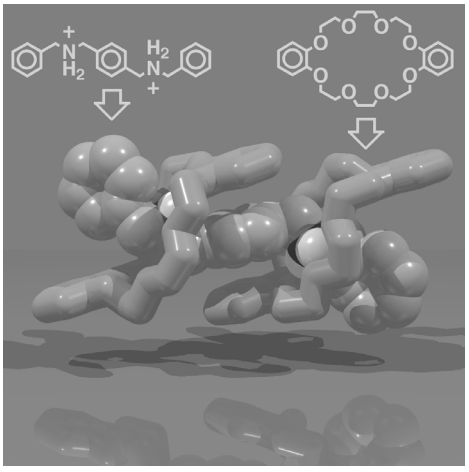

Figure 1.4. The solid-state superstructure of a [3]pseudorotaxane $[(DB24C8)_2 \cdot \mathbf{1}]^{2+}$ formed between a thread-like molecule ($\mathbf{1} \cdot 2PF_6$)—containing *two* ammonium centers—and *two* DB24C8 macrocycles.

desired complexes in which a full complement of crown ethers were found to encircle each of the extended DBA^+ homologues $\mathbf{1}$–$\mathbf{3} \cdot n PF_6$. Gratifyingly, the [3]pseudorotaxane $[(DB24C8)_2 \cdot \mathbf{1}][2PF_6]$ and [4]pseudorotaxane $[(DB24C8)_3 \cdot \mathbf{2}][3PF_6]$ were isolated as crystalline materials, which were subjected to X-ray analysis, confirming the integrity (Figures 1.4 and 1.5, respectively) of the NH_2^+/crown ether recognition in each case. In direct analogy with the interactions noted in the crystal structure of the parent [2]pseudorotaxane $[DB24C8 \cdot DBA][PF_6]$, the [3]pseudorotaxane $[(DB24C8)_2 \cdot \mathbf{1}][2PF_6]$ (Figure 1.4)[30,32] also appears to be stabilized *via* a combination of N^+–H···O and C–H···O hydrogen bonding interactions. In addition, one catechol ring from each of the centrosymmetrically related DB24C8 macrocycles participates in a π–π stacking interaction with the central aromatic ring of $\mathbf{1}^{2+}$. The X-ray crystal structure of the [4]pseudo-rotaxane $[(DB24C8)_3 \cdot \mathbf{2}][3PF_6]$ (Figure 1.5)[33] confirms, once again, that each NH_2^+ site on the thread ($\mathbf{2}^{3+}$) is encircled by a DB24C8 macrocycle as a consequence of the usual combination of

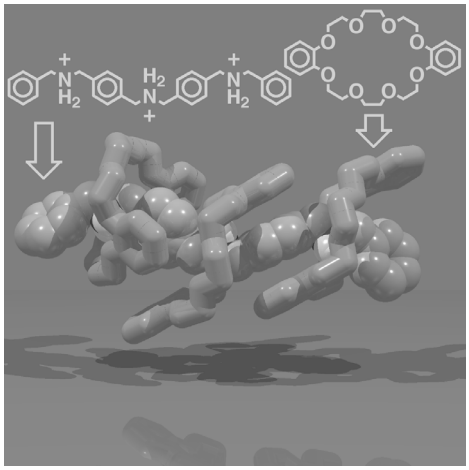

Figure 1.5. The solid-state superstructure of a [4]pseudorotaxane $[(DB24C8)_3 \cdot \mathbf{2}]^{3+}$ formed between a thread-like molecule ($\mathbf{2} \cdot 3PF_6$)—containing *three* ammonium centers—and *three* DB24C8 macrocycles.

N^+–H···O and C–H···O hydrogen bonding interactions. As before, additional stabilization is provided by supplemental π–π stacking interactions within this four-component supermolecule. Interestingly, in contrast with the [3]pseudorotaxane [$(DB24C8)_2$·**1**]-[$2PF_6$] in which there are no significant inter-supermolecule interactions, the [4]pseudorotaxane [$(DB24C8)_3$·**2**][$3PF_6$] forms π–π-linked dimers in the solid state giving rise, in principle, to a [7]pseudorotaxane.

Unfortunately, despite repeated efforts, a crystalline sample of the [5]pseudorotaxane was not obtained. However, solution and gas-phase investigations[33] of this system—employing ^{1}H NMR spectroscopy and FAB mass spectrometry, respectively—suggested strongly the formation of the five-component complex in which four DB24C8 rings are threaded onto the tetracation **3**$^{4+}$, encircling all of the NH_2^+ sites to afford a [5]pseudorotaxane. At this point, it can be concluded tentatively that, given a linear thread-like molecule containing *n* NH_2^+ sites, in all likelihood, under favorable conditions, *n* DB24C8 macrocycles will shuffle onto such a 'template', locating themselves such that each NH_2^+ center is encircled by one macrocycle.

Hence, predicting the nature of discrete superstructures, in this case, now appeared plausible. However, one aspect of the solid-state behavior of these complexes is still apparently random – as it stands, there appears to be no rhyme or reason as to how individual complexes pack with respect to one another. If we consider the extended solid-state superstructures of the [2]-, [3]-, and [4]pseudorotaxanes (*vide supra*), we note that each of them behaves differently. The [2]pseudorotaxane forms infinite, one-dimensional,

π–π-linked chains, the [3]pseudorotaxane appears to have no desire to interact outside of the discrete 2:1 supermolecule units, and the [4]pseudorotaxane forms π–π-linked dimers! Therefore, the next challenge was to try to address this issue, by controlling, in some fashion, interactions between discrete supermolecules.

1.4. Controlling the Extended Superstructure

Perhaps one of the most studied and well known[34] interactions in the field of crystal engineering is the carboxylic acid dimer supramolecular synthon. What makes this interaction so versatile, and hence so appealing, is the fact that its directionality can be controlled and/or influenced by subtle changes in the design of the species to which it is appended. This property can be exemplified by considering (Figure 1.6) three simple examples, namely (i) tere-phthalic acid,[35] (ii) isophthalic acid,[36] and (iii) 5-decyloxy-isophthalic acid.[37] When the two carboxylic acid groups are

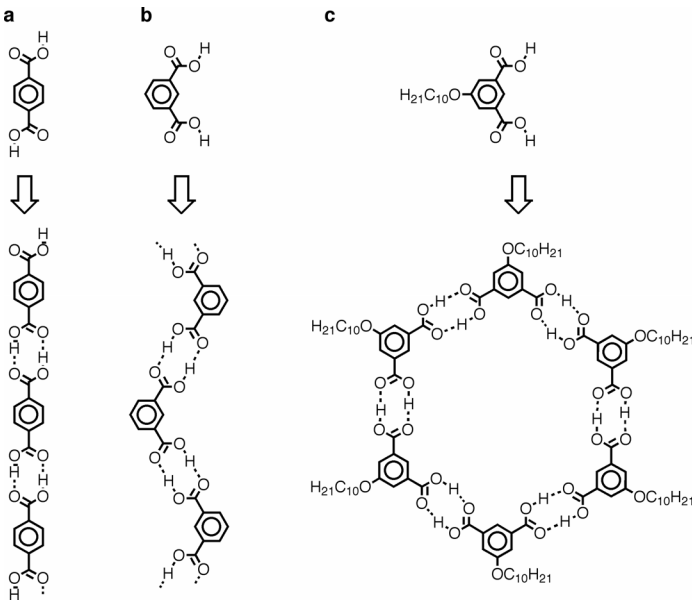

Figure 1.6. The influence of both directionality and steric crowding upon solid-state superstructures assembled *via* the carboxylic acid dimer are highlighted. The *para* disposition of carboxylic acid groups in terephthalic acid (**a**) results in the formation of infinite linear tapes, whereas the *meta* disposition—as in isophthalic acid (**b**)—produces a crinkled tape. The sterically congested 5-decyloxyisophthalic acid (**c**) is precluded from forming an extended tape superstructure, assembling instead into discrete hexameric supramacrocycles.

disposed *para* to one another on a benzene ring, as in terephthalic acid, the solid-state superstructure is that of a linear tape. By simply changing the substitution pattern to *meta*, as in isophthalic acid, the solid-state superstructure becomes reminiscent of a crinkled tape. Finally, introducing sterically demanding groups onto the isophthalic acid ring, as in the case of 5-decyloxyisophthalic acid, disfavors the formation of any kind of tape, and discrete supramolecular macrocycles are produced. With these observations in mind, Stoddart and coworkers set out[38] to marry together the $R_2NH_2^+$/DB24C8 recognition motif with that of the carboxyl dimer supramolecular synthon. An obvious condition is that a high degree of 'orthogonality' exists between the supramolecular synthons; *i.e.*, the carboxylic acid groups are required to form only dimers and each NH_2^+ site should be encircled by a DB24C8 macrocycle. In other words, these two supramolecular synthons must operate independently of one another – *i.e.*, crown ethers should thread onto their NH_2^+ sites oblivious to the formation of carboxyl dimers and *vice versa*.

The investigation began with the *covalent* syntheses of a range of carboxyl-substituted DBA·PF_6 derivatives (**4**–**7**·PF_6) (Chart 1.2) in which both (i) the number of CO_2H groups and (ii) their relative dispositions around the DBA^+ skeleton were varied. Each of these carboxyl-substituted thread compounds was mixed, in solution, with an equimolar quantity of DB24C8, thereby initiating

Compound	Structure
4·PF_6	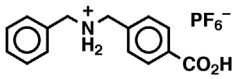
5·PF_6	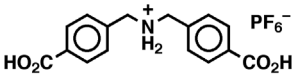
6·PF_6	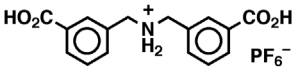
7·PF_6	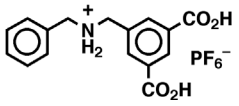

Chart 1.2

the *supramolecular* syntheses. From each of these solutions, good quality single crystals were obtained that were then subjected to X-ray analysis. In each case, the integrity of the $R_2NH_2^+$/DB24C8 recognition was maintained. The initial hypothesis—essentially that the carboxylic acid groups would not interfere with the threading process and *vice versa*—was correct. Hence, without exception, a [2]pseudorotaxane was formed in the solid state, accompanied by the now familiar combination of N^+–H···O and C–H···O hydrogen bonds, with, in some cases, supplemental π–π stacking interactions. More important, however, was this question: What role do the carboxyl groups play, if any, in orchestrating the overall arrangement of individual 1:1 complexes? Let us consider each superstructure in turn, focusing in particular upon the inter-[2]pseudorotaxane interactions arising from the presence of the carboxylic acid groups.

The X-ray crystallographic analysis of the 1:1 complex formed between DB24C8 and **4**·PF_6 confirmed (Figure 1.7) that the $\mathbf{4}^+$ cation is, as expected, threaded through the cavity of the DB24C8 macrocycle, affording the [2]pseudorotaxane [DB24C8·**4**][PF_6]. Further investigations revealed (Figure 1.8) that the individual 1:1 complexes are linked in a head-to-tail fashion, resulting in a supramolecular architecture that is somewhat reminiscent of a linear daisy chain[39,40] array. This extended superstructure arises as a consequence of the

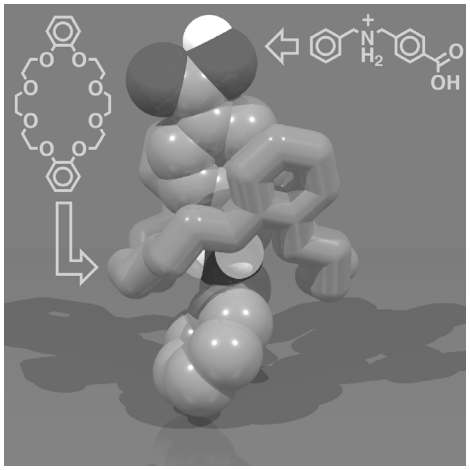

Figure 1.7. The solid-state superstructure of the [2]pseudorotaxane [DB24C8·**4**]$^+$ formed between the *para*-carboxylic acid-substituted DBA^+ cation $\mathbf{4}^+$ and DB24C8.

formation of bifurcated hydrogen bonds between the hydrogen atom of the carboxylic acid group present in $\mathbf{4}^+$, and both of the oxygen atoms of one of the catechol rings in the DB24C8 component of a neighboring [2]pseudorotaxane. Therefore, the formation of carboxyl dimers is, in this particular example, not a favorable process. The observations made on this superstructure highlight a very important point: they remind us that we still have a very long way to go in understanding the factors that affect solid state organization. As predicted, the NH_2^+ center finds itself encircled by a DB24C8 macrocycle. The subsequent head-to-head dimerization of these carboxyl-substituted [2]pseudorotaxanes—*via* the carboxyl dimer—would afford discrete four component supermolecules, possessing a [3]pseudorotaxane-like structure. It is now apparent, however, that the propensity for carboxyl dimer formation is influenced dramatically by the environment surrounding the carboxylic acid groups. In this superstructure, a head-to-head dimerization would result in the close contact of the DB24C8 rings in adjacent 1:1 complexes. This steric clash counters any enthalpic gain from carboxyl dimer formation, forcing the system to adopt an alternative, low energy arrangement – namely a head-to-tail-linked array. Such subtle effects are difficult to foresee. The next example serves to reinforce this point.

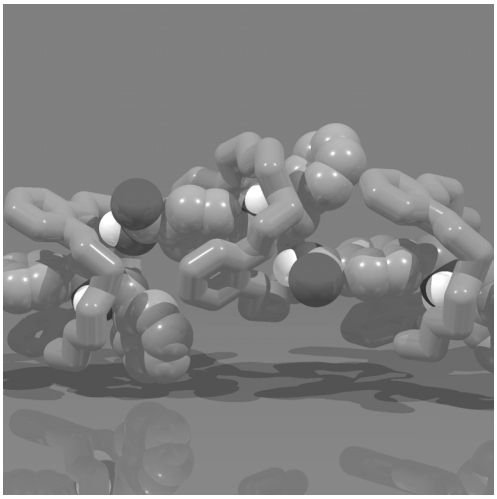

Figure 1.8. An infinite, linear, daisy chain-like array of $[DB24C8 \cdot \mathbf{4}]^+$ is formed as a result of hydrogen bonding between the carboxylic acid of one thread and the crown ether component of a neighboring [2]pseudo-rotaxane.

A logical extension of this project involved attaching one CO_2H group to *each* of the phenyl rings of the DBA^+ ion, resulting in $\mathbf{5}\cdot PF_6$. A reasonable expectation—one that arises from such a disposition of carboxyl groups about the DBA^+ framework—is the formation of a carboxyl dimer-linked tape of $\mathbf{5}^+$ cations, in which each NH_2^+ center is encircled by a DB24C8 macrocycle. Subsequent X-ray crystallographic analysis of the 1:1 complex formed between DB24C8 and $\mathbf{5}\cdot PF_6$ confirmed (Figure 1.9) that the $\mathbf{5}^+$ cation is indeed threaded through the cavity of the DB24C8 macrocycle, affording the [2]pseudorotaxane $[DB24C8\cdot\mathbf{5}][PF_6]$.

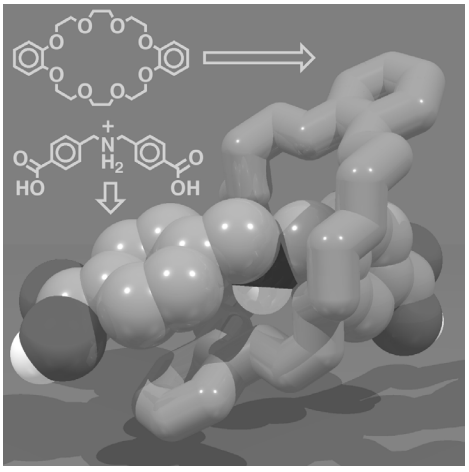

Figure 1.9. The solid-state superstructure of the [2]pseudorotaxane $[DB24C8\cdot\mathbf{5}]^+$ formed between the bis-*para*-carboxylic acid-substituted DBA^+ cation $\mathbf{5}^+$ and DB24C8.

Instead of the extended superstructure proposed above, however, the [2]pseudorotaxanes are observed (Figure 1.10) to dimerize *via* π–π stacking interactions. Further propagation of this dimeric superstructure *via* carboxyl dimer formation —between the 'free' carboxyl groups at the termini—is precluded by virtue of the formation of O–H···O hydrogen bonds between the carboxylic acid proton and the oxygen atom of included acetone molecules.

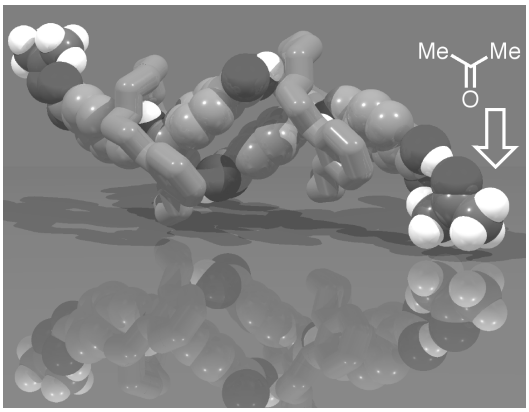

Figure 1.10. Despite the formation of a carboxylic acid dimer between individual [2]pseudorotaxanes, the possibility of an infinite hydrogen-bonded polymer is negated by the formation of hydrogen bonds between the terminal carboxylic acid protons and included acetone molecules in the solid-state superstructure of $[DB24C8\cdot\mathbf{5}]^+$.

Once again, the system conspires to produce a superstructure in which the anticipated carboxyl dimer supramolecular synthon is absent! Once more, the interaction, which is perhaps—on paper at least—the most obvious, is superseded by other significant noncovalent forces. At the risk of anthropomorphizing these molecules, it can be imagined that, given a choice, the building blocks will always choose to assemble into a minimum-energy structure. Although it is possible to tempt the building blocks into using one type of intermolecular interaction in preference to another—simply by incorporating the appropriate recognition motifs—only the building blocks themselves will know what the best *overall* combination of these stabilizing forces is. Unfortunately, one of the fundamental problems associated with crystal engineering is that each type of noncovalent interaction is essentially considered in isolation. Nonetheless, more analogues of this system were studied in order to gain a greater understanding of the factors at work.

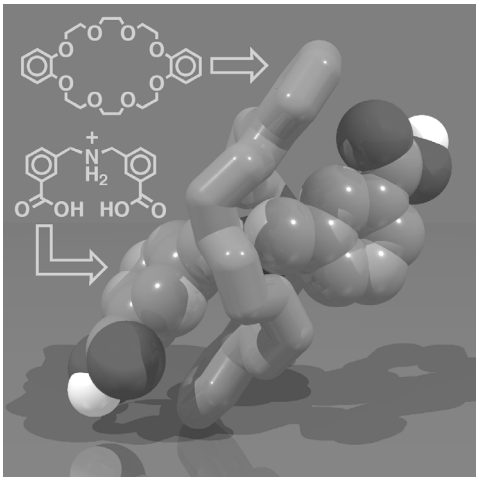

Figure 1.11. The solid-state superstructure of the [2]pseudorotaxane [DB24C8·**6**]$^+$ formed between the bis-*meta*-carboxylic acid-substituted DBA$^+$ cation **6**$^+$ and DB24C8.

In the next investigation, the focus fell upon the *meta*, *meta* disubstituted analogue of **5**·PF_6, namely **6**·PF_6. Since directionality is an important consideration when studying the carboxyl dimer, it was decided to examine the effect of this change in substitution pattern. The X-ray crystallographic analysis of the 1:1 complex formed between DB24C8 and **6**·PF_6 revealed (Figure 1.11) that the **6**$^+$ cation is again, as expected, threaded through the cavity of the

DB24C8 macrocycle, affording the [2]pseudorotaxane [DB24C8·**6**][PF_6]. For the first time in this series, the formation of carboxylic acid dimers was observed. The [2]pseudorotaxanes are linked together by virtue of carboxyl dimer formation, affording (Figure 1.12) an infinite, one-dimensional, main-chain pseudopolyrotaxane.[41] In this case, it appears that the conditions for the formation of carboxyl dimers are favorable. Specifically, the conformation of the DB24C8 macrocycle allows the linking of 1:1 complexes, in this fashion, without inducing any steric congestion of their catechol units, and, although acetone solvent molecules are present in the crystal lattice, they play no role in determining the extended superstructure. Therefore, it is possible to merge successfully different modes of molecular recognition in order to generate large, architecturally complex superstructures. Unfortunately, there is little control that can be exerted over the *self*-assembly[18] process, since the chemist's influence ends with the design and synthesis of the monomers. The best laid plans often do not work out. Little more can be done than to suggest a way in which the building blocks—the meccano—should organize themselves, and then see what happens. There are usually many subtle factors at work that are difficult, if not impossible, to compensate for within a system. This sentiment is best expressed with

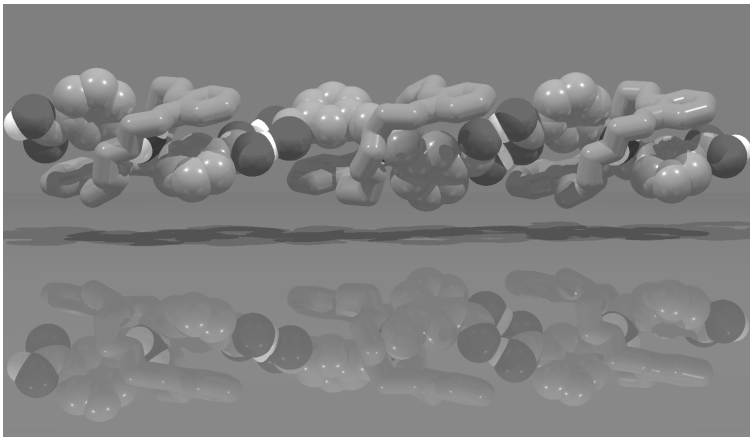

Figure 1.12. The X-ray crystallographic analysis of [DB24C8·**6**]-[PF_6] reveals the formation—in the solid state—of a carboxyl-dimer-linked main chain pseudopolyrotaxane.

two examples – namely (i) why, in some cases, does the crown ether adopt a conformation that makes carboxyl dimer formation unfavorable, *i.e.*, what does the system have to gain, and (ii) how do we know when solvent of crystallization will play a key role in determining the extended superstructure? These comments aside, the cause is not lost. If we are prepared to accept that the discipline of crystal engineering is—at this time at least—not an exact science, it is easy to see how it offers us a set of guidelines with respect to solid-state design. With this caveat in mind, let us continue our exploration in this field, by asking ourselves the question – what would be the effect of placing the two CO_2H groups on the same phenyl ring of the DBA^+ cation, as in **7**·PF_6?

Subsequently, the X-ray crystallographic analysis of the 1:1 complex formed between DB24C8 and **7**·PF_6 revealed (Figure 1.13) that the $\mathbf{7}^+$ cation is, as expected, threaded through the cavity of the DB24C8 macrocycle, affording the [2]pseudorotaxane [DB24C8·**7**][PF_6]. Furthermore, the packing of the 1:1 complexes reveals the formation (Figure 1.14) of a side-chain[41] pseudopolyrotaxane in which the adjacent [2]pseudorotaxane units are linked by virtue of carboxyl dimer formation, much as they are in [DB24C8·**6**][PF_6]. In summary, the feasibility of combining different molecular recognition motifs, *i.e.*, supramolecular synthons, for the construction of highly ordered interwoven

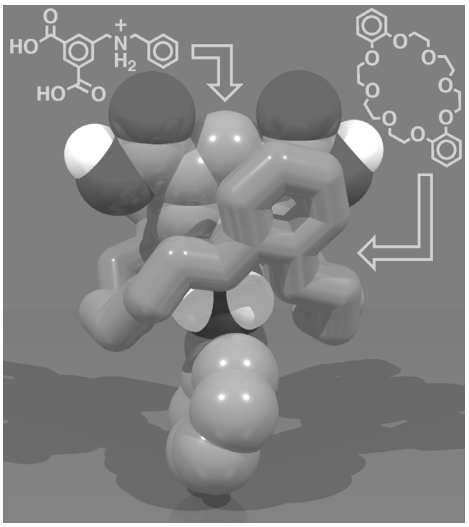

Figure 1.13. The solid-state superstructure of the [2]pseudorotaxane [DB24C8·**7**]$^+$ formed between the isophthalic acid-substituted DBA^+ cation $\mathbf{7}^+$ and DB24C8.

networks in the solid state, has been demonstrated. The $R_2NH_2^+$/crown ether recognition appears, so far, to be general, and persists despite the changes made elsewhere in the building blocks. In contrast, the carboxylic acid dimer is *not* always formed. Initially, perhaps, this result is a little surprising. However, once we cast aside our naïve expectations, it is easy to appreciate that many subtle factors can contribute to the formation of the observed crystalline superstructure.

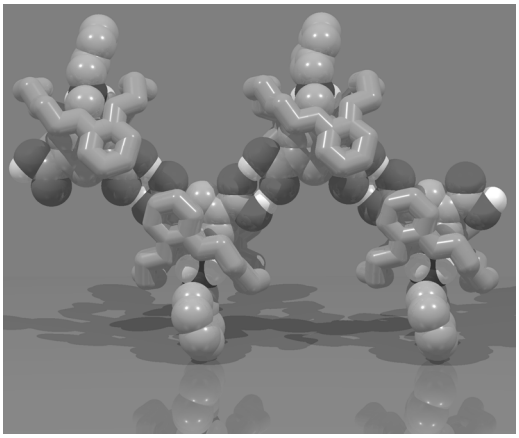

Figure 1.14. The side-chain pseudopoly-rotaxane formed as a result of carboxylic acid dimerization in the extended superstructure of $[DB24C8 \cdot \mathbf{7}]^+$.

1.5. Changing the Rings and Ringing the Changes

The recognition expressed between DB24C8 and $R_2NH_2^+$ ions has been exploited in the construction of many supramolecular and molecular systems – not just those highlighted so far. Not only have many interwoven complexes been generated as a result of *supramolecular synthesis*,[10] but the concept of *supramolecular assistance*[10] *to covalent synthesis* has also been employed in the creation of interlocked molecules.[20,21] Consequently, there are many examples of $R_2NH_2^+$/DB24C8-based rotaxanes[26,42] including, most recently, two examples[43] of molecular shuttles. So far, just one particular crown ether—namely DB24C8—has been considered. However, to create a molecular meccano set capable of generating a diverse range of 'structures', this singular selection of

macrocyclic component is somewhat limiting. Consequently, the following sections will describe the consequences—to $R_2NH_2^+$ ion/crown ether recognition—of (i) changing the groups appended to the basic [24]crown-8 framework and (ii) expanding the size of the macrocyclic ring.

1.5.1. Tetrabenzo[24]crown-8 (TB24C8)

As part of ongoing investigations, the consequences[44] (Chart 1.3) of either adding, or removing, aromatic units from the [24]crown-8 skeleton present in DB24C8 were investigated. Removal of one aromatic ring affords benzo[24]crown-8 (B24C8) while removal of both results in the wholly aliphatic compound [24]crown-8 (24C8). On the other hand, the addition of two aromatic rings results[45] in tetrabenzo-[24]crown-8 (TB24C8), a crown ether in which all eight oxygen atoms are of the less basic phenolic type. The two former compounds—namely B24C8 and 24C8—were observed to thread onto NH_2^+ ion-containing molecules affording pseudo-rotaxanes in direct analogy with the behavior observed for DB24C8. Although, in these cases, no solid-state structures could be

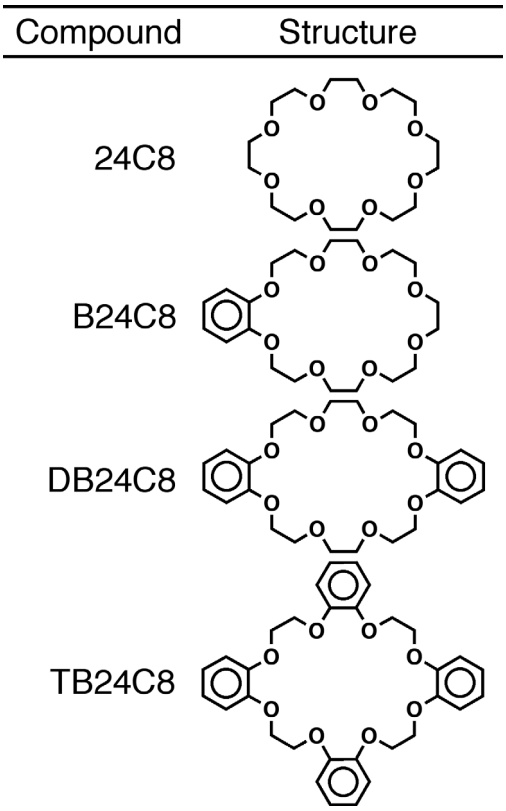

Chart 1.3

obtained, there was overwhelming solution and gas-phase evidence supporting the threading process. However, in contrast with these two well-behaved [24]crown-8-derived macrocycles, TB24C8 seemed to have no desire to include within its macrocyclic cavity an $R_2NH_2^+$ ion, at least as evidenced by both solution-state studies (^{1}H NMR spectroscopy) and gas-phase investigations (FABMS). Initially, this conclusion was reinforced by solid-state studies[46] of crystals grown from solutions containing equimolar quantities of TB24C8 and DBA·PF_6.

X-Ray analysis of crystals obtained from an MeCN/Et_2O solution revealed[47] the formation of a TB24C8 bis-MeCN clathrate (Figure 1.15), whereas crystals grown from a $CHCl_3$/Et_2O were shown[48] to consist of 'free' TB24C8 molecules (Figure 1.16). In each case, despite markedly different crown ether conformations, extended superstructures are formed in which adjacent TB24C8 molecules are linked *via* networks of C–H···π interactions.[14] However, perhaps the most important aspect of these two structures is the absence of DBA·PF_6 – *i.e.*, in each case, the crown ether prefers to crystallize alone or with solvent. Therefore, all efforts seemed to indicate that the TB24C8/DBA^+ interaction is very weak. Consequently, results[49] of the X-ray structural analysis of a third set of crystalline material—this time grown from a 1:1 mixture of the components in

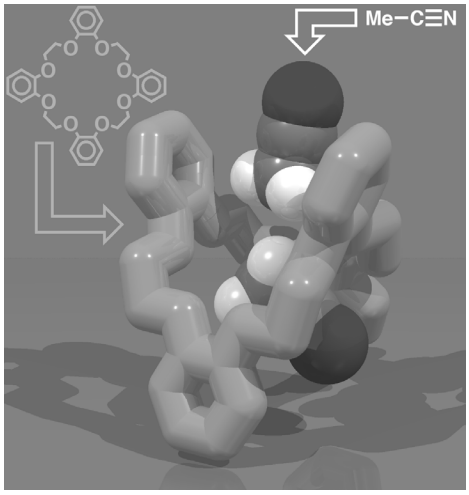

Figure 1.15. When grown from a MeCN/Et_2O solution, crystals of TB24C8 can be seen to contain enclathrated acetonitrile molecules.

$CHCl_3$/MeCN/*n*-C_6H_{14} solution—were greeted with a certain degree of surprise. This structure (Figure 1.17) not only has a 1:1 stoichiometry of TB24C8 and DBA·PF_6, but the DBA^+ cation is indeed threaded through the macrocyclic cavity of the crown ether, affording a [2]pseudorotaxane [TB24C8·DBA][PF_6], that is held together by N^+–H···O and C–H···O hydrogen bonds, with a supplemental π–π stacking interaction also contributing. In effect, the same interactions that govern the threading of a DBA^+ cation through a DB24C8 macroring are at work here. However, the most striking feature associated with the crystal superstructure (Figure 1.18) of [TB24C8·DBA][PF_6] concerns the PF_6^- anions. The 1:1 complexes (there are four independent [2]pseudorotaxanes in the asymmetric unit) are organized around a matrix of highly ordered PF_6^- anions, which appear to stabilize the crystal

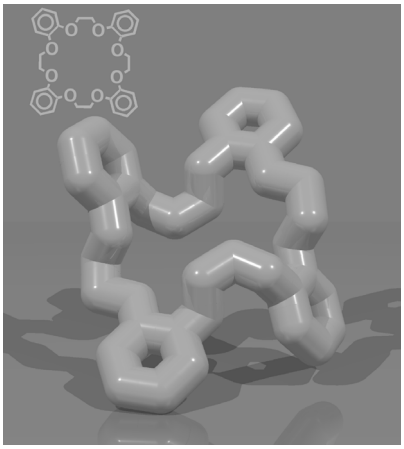

Figure 1.16. In the absence of MeCN, TB24C8 crystallizes without ordered solvent molecules.

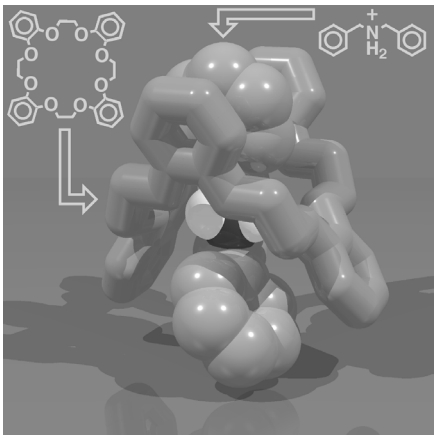

Figure 1.17. One of the four crystallographically independent superstructures with a [2]pseudorotaxane geometry observed in the X-ray analysis of [TB24C8·DBA][PF_6].

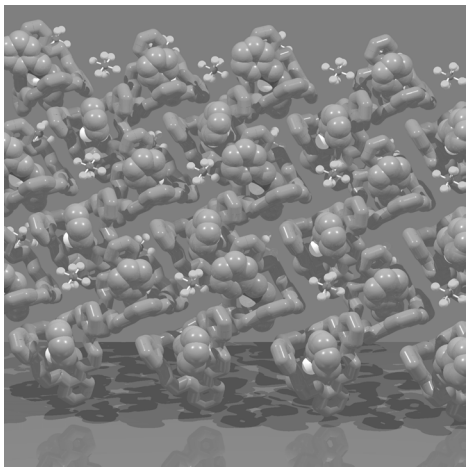

Figure 1.18. The extensively C–H···F hydrogen bond-stabilized extended superstructure of the complex [TB24C8·DBA]-[PF_6].

lattice *via* a myriad of C–H···F hydrogen bonding interactions.[50] Presumably, the unusual lack of disorder in these anions reflects their role in directing the kinetic assembly of this particular superstructure in the solid state. Therefore, although the threading of a DBA^+ cation through the cavity of a TB24C8 macrocycle is, in solution, not a thermodynamically favored process, the act of crystallization—an inherently kinetic event—favors, in the presence of PF_6^- anions, the formation of [2]pseudorotaxanes. This example is the first of many in this Chapter which will serve to highlight the pivotal role that PF_6^- anions can play in the solid-state synthesis of interwoven supramolecular arrays.

1.5.2. Benzometaphenylene[25]crown-8 (BMP25C8)

Although the $R_2NH_2^+$ ion/DB24C8 recognition motif has turned out to be particularly effective for the construction of interwoven arrays and interlocked molecules, it is not without its problems. Functionalization of the aromatic rings of DB24C8 renders the faces of such a substituted macrocycle enantiotopic. Consequently, the threading of an unsymmetrical NH_2^+-containing ion through the cavity of such a crown ether leads to the formation of diastereoisomeric complexes. Therefore, in creating a system that is rich in interlocked/interwoven motifs, it is possible that a mixture of stereoisomeric complexes may be formed. However, replacing one of the catechol rings of DB24C8 with a resorcinol ring alleviates this problem since substitution at the 5-position of the resorcinol ring does not desymmetrize the molecule. Obviously, however, this strategy[51] is only

worthwhile if such a modification does not reduce the macrocycle's propensity for binding $R_2NH_2^+$ ions.

Investigations[51] into the solid-state superstructure of a 1:1 complex formed between BMP25C8 and DBA·PF_6 revealed (Figure 1.19) the formation of a [2]pseudorotaxane [BMP25C8·DBA][PF_6]. The DBA^+ cation is threaded through the cavity of the BMP25C8 macroring, and the complex is stabilized as a result of N^+–H···O hydrogen bonding – there are no short C–H···O contacts present in this superstructure. In addition, there is a supplemental π–π stacking interaction observed between the thread and crown ether components. Individual [2]pseudorotaxanes are organized into sheets (Figure 1.20) as a consequence of inter-complex π–π and C–H···π interactions. Thus, it has been demonstrated that this relatively small change in crown ether constitution does not preclude the formation of threaded complexes. Consequently, it can be noted that the molecular meccano kit is slowly expanding. In an effort to characterize, as fully as

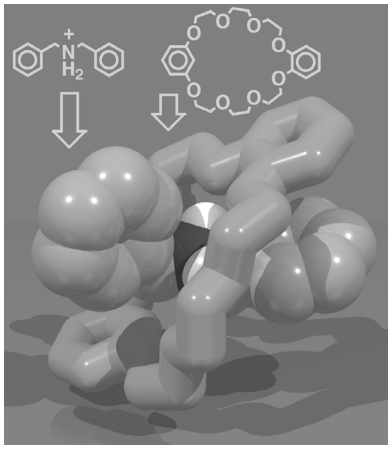

Figure 1.19. The solid-state superstructure of the [2]pseudorotaxane [BMP25C8·DBA]$^+$ formed between the DBA^+ cation and BMP25C8.

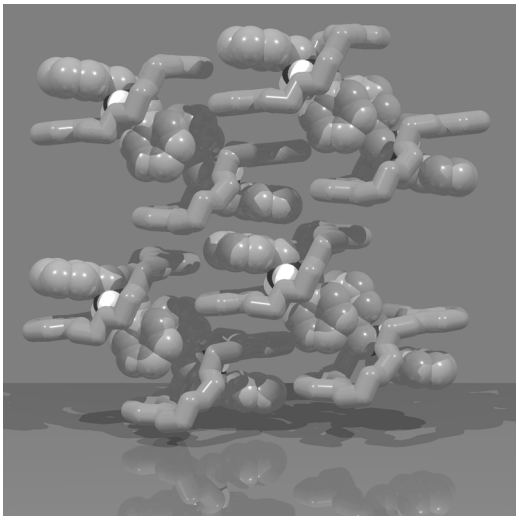

Figure 1.20. Discrete [BMP25C8·DBA]$^+$ supermolecules are linked in the solid state to form extended sheets.

possible, all of the building blocks in the meccano set, the X-ray crystal structure of 'free' BMP25C8 was also determined (Figure 1.21), revealing the formation (Figure 1.22) of a constricted nanotube in which the molecules stack one on top of the other. The primary interactions governing this assembly are C–H···π hydrogen bonds—originating from the phenoxymethylene hydrogen atoms of both the resorcinol and catechol rings—which are supplemented, to a lesser degree, by partial overlap of both the catechol and resorcinol rings of adjacent molecules within the stack.

Figure 1.21. The solid-state structure of BMP25C8.

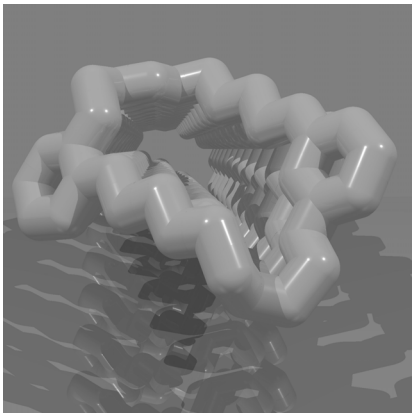

Figure 1.22. Constricted nanotubes —stabilized by intermolecular C–H···O hydrogen bonds—are formed by the stacking of BMP25C8 molecules in the solid state.

1.5.3. Tribenzo[27]crown-9 (TB27C9)

To create higher-order supramolecular architectures, it becomes apparent that the potential for modification of both the thread and crown ether components is desirable. The placement of additional recognition sites at the termini of the $R_2NH_2^+$ ions has already been discussed. Recall the use of CO_2H groups, which resulted in the formation of interesting extended superstructures. Ultimately, the functionalization of the crown ether components is a realistic goal. However, placing substituents on the aromatic rings of the DB24C8 macrocycle only presents the opportunity of disposing functional groups 180° apart.

With the goal of expanding the molecular meccano kit even further, a crown ether with three-fold symmetry was investigated,[52] namely tribenzo-[27]crown-9 (TB27C9), which—in the fullness of time—should allow us to present additional recognition sites at 120° angles. The X-ray crystallographic analysis of the solid-state superstructure of a 1:1 complex formed between TB27C9 and (p-CO_2Me)$_2$-DBA·PF_6 revealed (Figure 1.23) the formation of a [2]pseudorotaxane [TB27C9·(p-CO_2Me)$_2$-DBA][PF_6]. The $R_2NH_2^+$ ion is threaded through the cavity of the TB27C9 macroring and the complex is stabilized by N^+–H···O hydrogen bonding. Although there are no short C–H···O contacts observed in this superstructure, a supplemental π–π stacking interaction is observed between the thread and crown ether components. Additionally, probing of the inter-[2]pseudorotaxane interactions (Figure 1.24) revealed the formation of C–H···π-linked sheets. Therefore, it is now possible to generate interwoven $R_2NH_2^+$ ion-based superstructures, utilizing a variety of

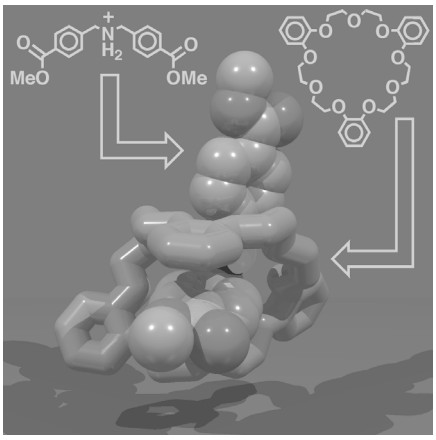

Figure 1.23. The solid-state superstructure of the [2]pseudorotaxane [TB27C9·(p-CO_2Me)$_2$-DBA]$^+$ formed between the p-CO_2Me-disubstituted DBA^+ cation and TB27C9.

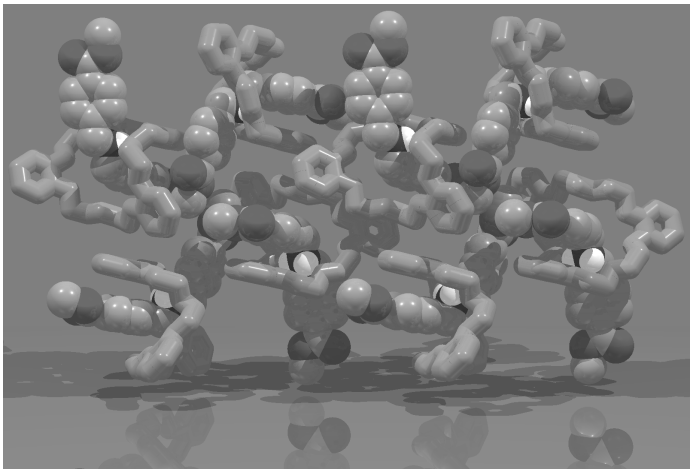

Figure 1.24. The extended superstructure of [TB27C9·(p-CO_2Me)$_2$-DBA][PF_6] consists of extended sheets that are stabilized by inter-[2]pseudorotaxane C–H···π hydrogen bonds.

crown ethers, not only those with [24]crown-8 constitutions, but also those involving [25]crown-8 and [27]crown-9 macrorings. Thus, as the molecular meccano kit grows, the mixing and matching of crown ethers with $R_2NH_2^+$ ions—in an effort to influence the assembly of the final superstructure—can be envisaged. Each building block—with its own distinctive particular attributes—can be chosen with the intention of directing the formation of higher-order superstructures in a deliberate manner.

1.5.4. Bisparaphenylene[34]crown-10 (BPP34C10)

Upon further expansion of the cavity size of a crown ether to 34 atoms, as in bisparaphenylene[34]crown-10 (BPP34C10), the threading of two DBA^+ cations through the macrocyclic polyether is observed.[30,32] In this particular ditopic crown ether, the two polyether loops are separated to such an extent that each arc can satisfy the hydrogen bonding requirements of a DBA^+ cation. The X-ray crystallographic analysis of the solid-state superstructure of a 1:2 complex formed between BPP34C10 and $DBA{\cdot}PF_6$ reveals (Figure 1.25) the formation of a *double-stranded* [3]pseudorotaxane $[BPP34C10{\cdot}(DBA)_2][2PF_6]$. Two DBA^+ ions are threaded simultaneously through the cavity of the BPP34C10 macroring and the complex is stabilized principally by N^+–H···O hydrogen

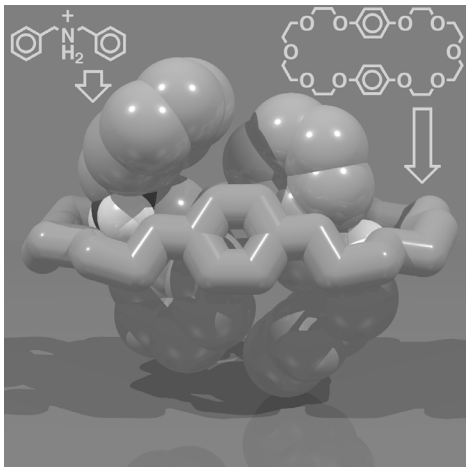

Figure 1.25. The solid-state superstructure of a *double-stranded* [3]pseudorotaxane $[BPP34C10{\cdot}(DBA)_2]^{2+}$ formed between BPP34C10 and $DBA{\cdot}PF_6$.

bonding. Although there are no short C–H···O contacts observed in this superstructure, additional stabilization arises from the formation of edge-to-face aromatic interactions (C–H···π bonds) between one phenyl ring in each DBA^+ cation and the hydroquinone rings of the macrocycle.

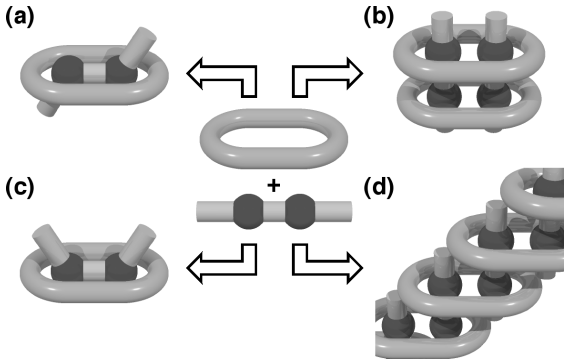

Figure 1.26. Conceivably, there are four possible distinct superstructures that may form upon co-crystallization of BPP34C10 and **1**·2PF_6: (**a**) a *single-threaded, double-docked* [2]pseudorotaxane, (**b**) a *double-threaded, double-encircled* [4]pseudorotaxane, (**c**) a face-to-face complex, and (**d**) a polymer.

In the knowledge that a BPP34C10 macrocycle can accommodate simultaneously two $R_2NH_2^+$ ions, the following question was posed – what type of superstructure could be formed by mixing BPP34C10 with a thread-like molecule containing two NH_2^+ centers, namely **1**·2PF_6? In theory, there are four possible superstructures (Figure 1.26) that one could reasonably expect to be formed as a result of satisfying the principle of maximal site occupancy.[53] In practice, the X-ray structural analysis[30] of crystals obtained from an Me_2CO/*n*-C_5H_{12} solution, containing a 1:1 mixture of BPP34C10 and **1**·2PF_6, revealed (Figure 1.27) the formation of the *double-*

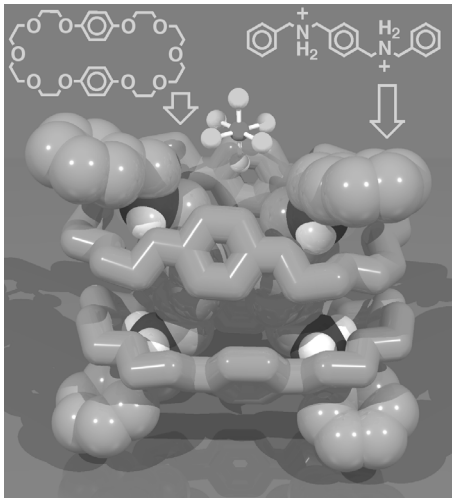

Figure 1.27. The solid-state superstructure of the *double-threaded, double-encircled* [4]pseudorotaxane $[(BPP34C10)_2\cdot(\mathbf{1})_2]^{4+}$ formed between BPP34C10 and $\mathbf{1}^{2+}$.

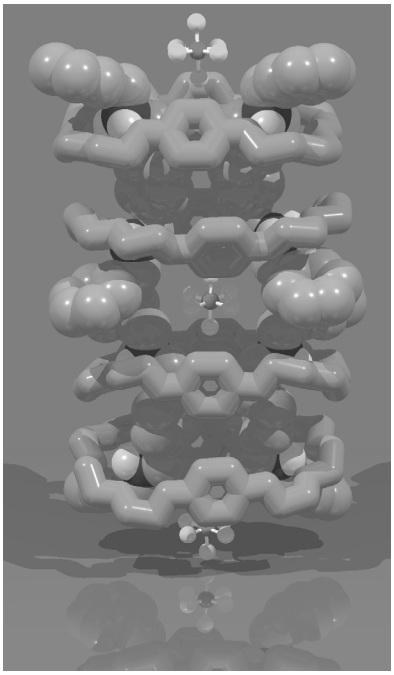

Figure 1.28. Individual [2 + 2] superbundles form columns in the solid state. The interstitial PF_6^- anions may play some role in the assembly of this infinite one-dimensional array.

encircled, *double-stranded* four-component superstructure $[(BPP34C10)_2 \cdot (\mathbf{1})_2][4PF_6]$. Each 2:2 complex is stabilized as a result of the formation of fourteen hydrogen bonding interactions – ten N^+–H···O and four C–H···O close contacts are observed. A closer examination of the solid-state superstructure revealed the presence of highly ordered PF_6^- anions situated at the termini of this supramolecular bundle. These PF_6^- anions enter into C–H···F hydrogen bonding interactions[50] with the two adjacent 2:2 complexes and may be responsible for the formation (Figure 1.28) of the one-dimensional array that propagates throughout the crystal lattice. So yet again, we see a clear indication that the counterions associated with the $R_2NH_2^+$ cations can influence, in some manner, the solid-state assembly of their interwoven superstructures with crown ethers. In essence, this section demonstrates the ability to tie together two NH_2^+ centers by encircling them with BPP34C10. Next, this new-found paradigm was exploited for the construction of other, more elaborate, interwoven supramolecular bundles.

1.6. Supramolecular Bundles

The logical, incremental approach adopted in this study had so far proved successful. From crown ethers that only accommodate *one* NH_2^+ center, one can move onto those

that will welcome *two* at once. Furthermore, the knowledge that *one* BPP34C10 macrocycle will tie together two *mono*cations led to the discovery that *two* BPP34C10 molecules will tie together two *di*cations. From these observations it is possible to deduce a simple algorithm that correlates with the solid-state self-assembly, that is – *n* BPP34C10 macrocycles will—by virtue of their ditopic nature—tie together two cationic species that each contain *n* NH_2^+ centers. For example, when BPP34C10 was mixed with the trifurcated trisammonium salt **8**·3PF_6, crystals were obtained[54] which were shown (Figure 1.29)—by X-ray crystallographic analysis—to consist of the five-component superbundle in which *three* BPP34C10 macrocycles tie together *two* trifurcated triscations. This superstructure is stabilized by the now customary N^+–H···O hydrogen bonding interactions; no close C–H···O contacts are observed. The mean interplanar separation of the two 1,3,5-triarylbenzene rings is approximately 4 Å and does not, therefore, represent a significant π–π interaction. Adjacent superbundles are rotated by 60° with respect to each other, and form (Figure 1.30) an interleaved one-dimensional array. The self-assembly of this [3 + 2] superbundle is remarkable in that this architecture is just one of many superstructures that could possibly be formed. However, this discrete—or closed—assembly not only satisfies the maximal site occupancy principle,[53] but it is also favored on entropic grounds. The formation of a porous, three-

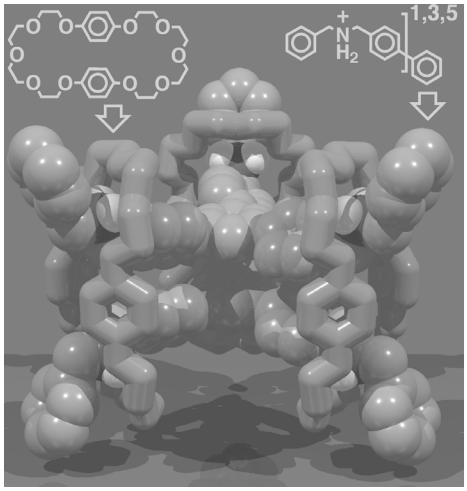

Figure 1.29. The solid-state superstructure of the five-component superbundle $[(BPP34C10)_3\cdot(\mathbf{8})_2]^{6+}$ formed between the trifurcated tris-ammonium cation $\mathbf{8}^{3+}$ and the ditopic crown ether BPP34C10.

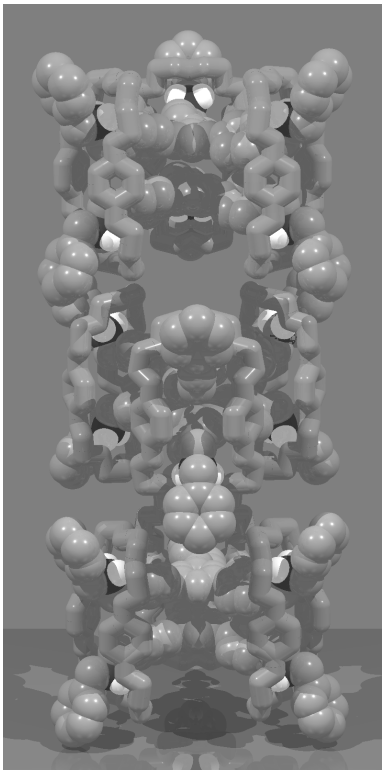

Figure 1.30. Interleaved one-dimensional arrays of the five component superbundle $[(BPP\text{-}34C10)_3\cdot(\mathbf{8})_2]^{6+}$ are formed in the solid state.

dimensional, supramolecular array—in which each BPP34C10 ring links an $\mathbf{8}^{3+}$ cation to three different $\mathbf{8}^{3+}$ cations—is also conceivable. However, such a process would be commensurate with a considerable loss of entropy, much more so than upon assembly of discrete [3 + 2] superbundles.

Using the now-established protocol, the next step was to synthesize[55] noncovalently a supramolecular analogue[56] of the photosynthetic special pair.[57] Conceptually, this task simply involved the extrapolation of the self-assembly algorithm from [2 + 2] and [3 + 2] superbundles to a [4 + 2] superbundle. It was anticipated that, by appending four DBA^+ ion-containing side chains onto a porphyrin core, a superstructure would be observed in which two of these tetrafurcated tetrakiscations would be tied together by four BPP34C10 macrocycles. This interwoven six-component architecture would require the co-facial stacking of the two porphyrin nuclei much like that observed in the case of the special pair located in the photosynthetic reaction center. Indeed, the X-ray crystallographic analysis of the 4:2 complex—formed between BPP34C10 and $\mathbf{9}\cdot 4PF_6$—revealed (Figure 1.31) the formation of the desired [4 + 2] superbundle, validating the design strategy. The bundle is once again stabilized by the usual N^+–H···O and C–H···O hydrogen bonding interactions, in addition to a π–π stacking

interaction between the porphyrin nuclei (mean interplanar separation = 3.65 Å). The relative dispositions of the porphyrin nuclei—similar to those observed in the photosynthetic reaction center—involve a sheared relationship in which the copper atoms are offset laterally by 3.05 Å and the Cu···Cu separation is 4.76 Å. The assembly of the six-component superbundle also occurs in solution as detected by EPR spectroscopy. In the absence of BPP34C10, EPR spectroscopy reveals that there are no interactions between the porphyrin nuclei. However, upon the addition of two equivalents of BPP34C10 to this solution, electronic coupling of copper centers is observed in the EPR spectrum, indicating the formation of BPP34C10-induced aggregates – presumably the [4 + 2] superbundle.

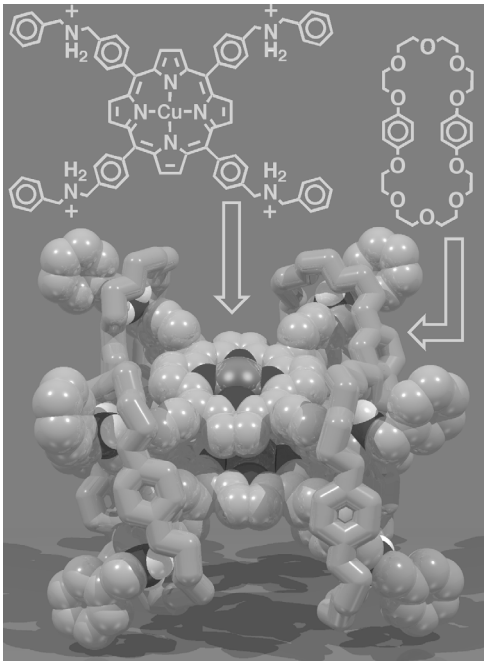

Figure 1.31. Co-crystallization of BPP34C10 and **9**·4PF_6 affords a six-component superbundle that is a supramolecular analogue of the photosynthetic special pair.

The formation of bundles is possible by employing crown ethers that possess more than one site capable of binding an $R_2NH_2^+$ ion. To date, this requirement has prevented the use of the parent system – namely the DB24C8/$R_2NH_2^+$ ion recognition motif. However, if it were possible to display *n* DB24C8 macrocycles about a core in a controlled fashion, and do likewise with *n* DBA^+ cations, the formation of superbundles is certainly possible. Already in hand was the trifurcated trisammonium salt **8**·3PF_6, and

so all that was required[58] was the design and synthesis of a complementary tris-DB24C8 derivative. The crown ether system was based upon a triphenylene core, and resulted in the tritopic receptor **11** in which three DB24C8 rings are displayed in a trigonal fashion.

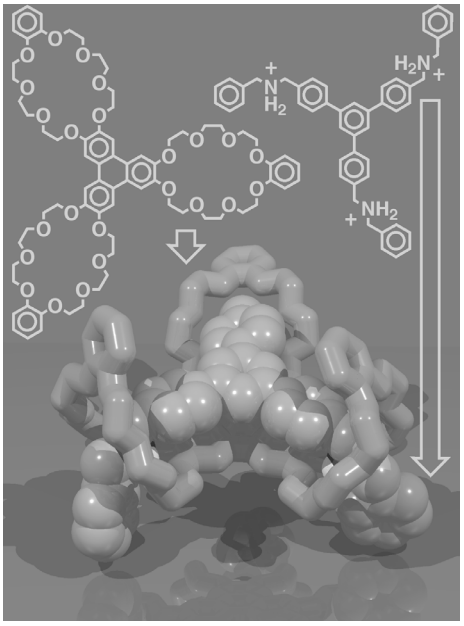

Figure 1.32. The solid-state superstructure of a *triple-threaded* 1:1 complex formed between a trifurcated trisammonium thread and a complementary triphenylene-based tris-DB24C8 derivative.

The X-ray crystallographic analysis of the 1:1 complex formed between the tris-crown ether **11** and **8**·3PF_6 revealed (Figure 1.32) the formation of the *triple-threaded* two-component superbundle. The noncovalent synthesis of this discrete superstructure presumably occurs as a consequence of the highly complementary nature of the two building blocks. Not only is complex stabilization achieved through the formation of N^+–H···O hydrogen bonds, but also by a π–π stacking of the aromatic cores (centroid-centroid separation = 3.6 Å). The solid-state behavior of these two components is mirrored in solution, wherein a very stable 1:1 complex—the triple-threaded superbundle—is observed.

1.7. Mixing and Matching

It has been proven consistently that two $R_2NH_2^+$ ions will thread simultaneously through the cavity of a BPP34C10 macrocycle. It has also been shown how the carboxyl dimer—in some cases—can be used to induce long range order in the overall crystalline

superstructures. To demonstrate the modular nature of the building blocks in the molecular meccano kit, an investigation[38] into the interaction of the carboxylic acid-substituted DBA^+ cations—only previously mixed with the monotopic receptor DB24C8—with the ditopic receptor, namely BPP34C10, was undertaken. The X-ray crystallographic analysis of the 1:2 complex, formed between BPP34C10 and **4**·PF_6 revealed (Figure 1.33) that, perhaps not surprisingly, *two* of the $\mathbf{4}^+$ cations find themselves encircled by a BPP34C10 macrocycle. The threading occurs in a co-directional manner, resulting in both carboxyl groups pointing in the same direction. This double-stranded [3]pseudorotaxane is stabilized by the formation of N^+–H···O hydrogen bonds – there are no close C–H···O contacts. Interestingly, the PF_6^- anion, once again, appears to play an important role in determining the superstructure. Located inbetween the cleft—formed by the two unsubstituted phenyl rings of the $R_2NH_2^+$ cations—is one of the fluorine atoms of the anion, from which there appears to be a close contact with a hydrogen atom from one of the threaded cations. Another close contact was observed between one of the other fluorine atoms of the anion and a hydrogen atom from the hydroquinone ring of BPP34C10. These close contacts may represent C–H···F hydrogen bonding[50] interactions, which, in turn, may dictate the co-directional manner in which the threads align themselves through the center of the crown ether. Consequently, the formation of

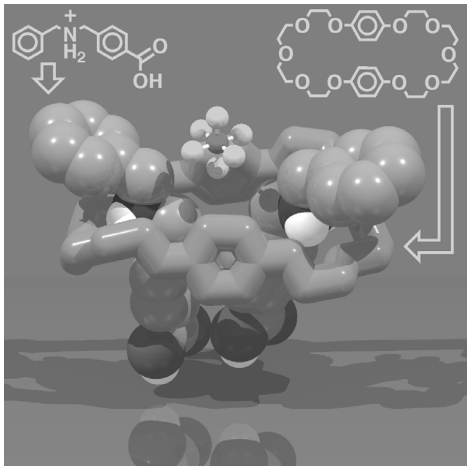

Figure 1.33. In a manner analogous to DBA·PF_6, **4**·PF_6 forms a *double-threaded* [3]pseudorotaxane when co-crystallized with BPP34C10.

an extended, carboxyl dimer-linked superstructure is precluded as the preferred mode of inter-superstructure interaction is the dimerization (Figure 1.34) of these [3]pseudorotaxanes. This six-component superstructure is highly reminiscent of the doubly-encircled double-threaded superstructure formed[32] between BPP34C10 and **1**·2PF_6. In essence, the carboxyl dimer supramolecular synthon is acting as a surrogate for a *p*-disubstituted phenyl ring.

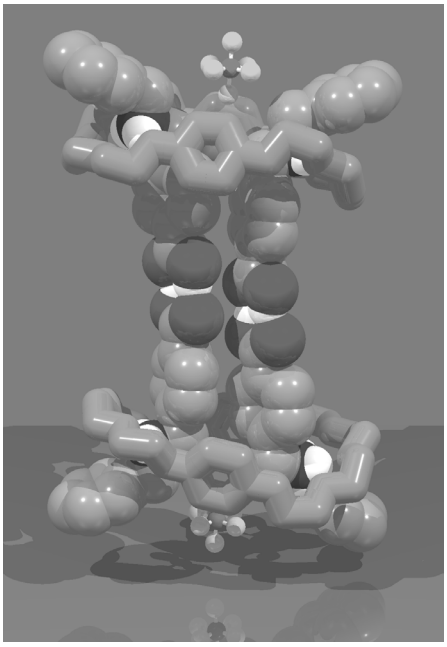

Figure 1.34. Individual [BPP34C10·(**4**)$_2$][2PF_6] [3]pseudorotaxanes dimerize in the solid state *via* the formation of carboxylic acid dimers.

The X-ray crystallographic analysis of the 1:2 complex formed between BPP34C10 and **10**·PF_6 (the *meta* analogue of **4**·PF_6) revealed (Figure 1.35) the formation of a superstructure that is very similar to that observed for [BPP34C10·(**4**)$_2$]$^{2+}$. Once again, the threading of the two cations is co-directional, and appears to result as a consequence of interactions with a similarly located PF_6^- anion. Complex stabilization is achieved in the same manner as before – namely by N^+–H···O hydrogen bonding, with no close C–H···O contacts observed. Once again, the individual [3]pseudorotaxanes dimerize noncovalently (Figure 1.36) by virtue of

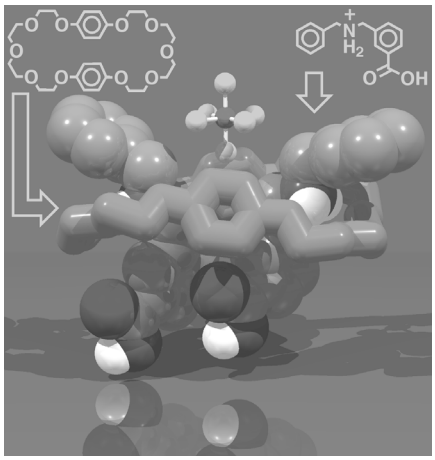

Figure 1.35. Similarly to **4**·PF_6, its *meta*-substituted cousin **10**·PF_6 forms a 1:2 complex when co-crystallized with BPP34C10.

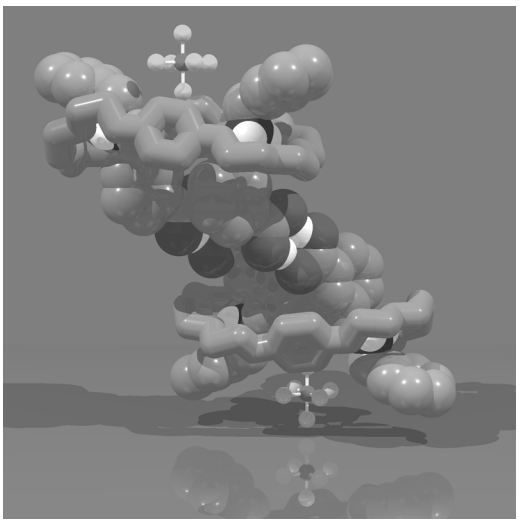

Figure 1.36. Discrete [BPP34C10·(**10**)$_2$][2PF$_6$] supermolecules dimerize—in the solid-state—as a result of carboxyl dimer formation.

carboxyl dimer formation. The recurrence of a selective positioning of one of the PF_6^- anions reinforces the belief that the anion plays a role in determining the co-directional manner in which the cations align themselves. In turn, this arrangement results in the carboxyl dimer-linked six-component supermolecules observed in these two examples, demonstrating just how the counterion can affect the overall solid-state superstructure.

In contrast, the X-ray crystallographic analysis of the 1:2 complex formed between BPP34C10 and the isophthalic acid-substituted cation **7**$^+$ revealed (Figure 1.37) the formation of a double-stranded [3]pseudorotaxane in which the two **7**$^+$ cations are threaded *centrosymmetrically* through the crown ether. As expected, this three component supermolecule is stabilized as a result of N$^+$–H···O hydrogen bonding interactions. Apparently, in this case, the PF_6^- anions do not participate actively in the solid-state assembly process, allowing for this head-to-tail threading of the $R_2NH_2^+$ ions. Now

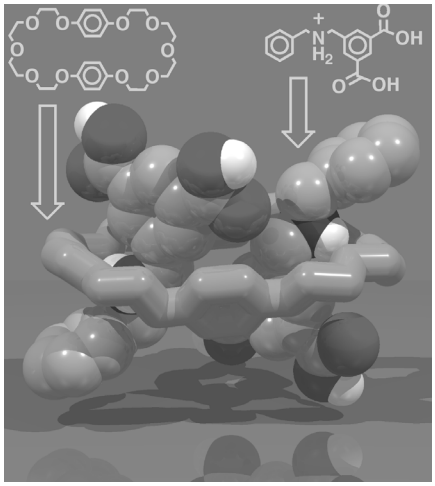

Figure 1.37. Two **7**$^+$ cations thread through the cavity of BPP34C10 in a centrosymmetric fashion, resulting in the formation of a [3]pseudorotaxane [BPP34C10·(**7**)$_2$]$^{2+}$ in the solid state.

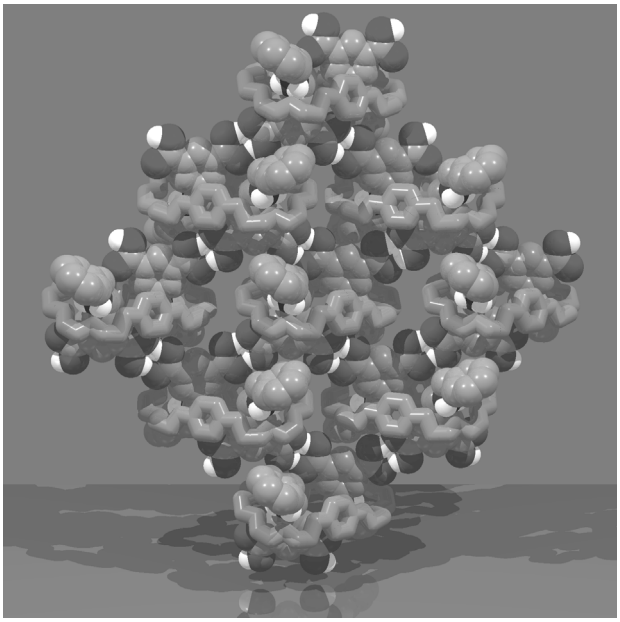

Figure 1.38. Analysis of the extended solid-state superstructure adopted by $[BPP34C10\cdot(\mathbf{7})_2]^{2+}$ reveals the existence of an interwoven cross-linked supramolecular polymer.

that the two carboxyl groups present in each [3]pseudorotaxane are aligned in opposite directions, on opposing sides of the macrocycle, discrete dimerization is precluded. Instead, multiple carboxyl dimer formation results in the formation (Figure 1.38) of an interwoven supramolecular cross-linked polymer. It has thus been demonstrated that it is possible to mix and match building blocks: the molecular meccano kit is truly modular in design, allowing for the combination of orthogonal supramolecular synthons for the fabrication of interwoven superstructures, the architectures of which, to some extent, can be controlled, by judicious choice of both crown ether and $R_2NH_2^+$ ion.

1.8. How Large can these Superstructures be?

Once it was noted that BPP34C10 can, with its two polyether loops, reliably complex with two equivalents of $DBA\cdot PF_6$ or structural analogues thereof, the question of utilizing larger crown ethers arose. Could larger macrocyclic polyethers—comprised of more than two polyether loops—accommodate[33,59] even more $R_2NH_2^+$ ions within their macrocyclic cavities? Preliminary extraction experiments suggested that the crown ethers

trisparaphenylene[51]crown-15 (TPP51C15) and tetrakisparaphenylene[68]crown-20 (TPP68C20) were capable of solubilizing, in CD_2Cl_2, three and four equivalents of $DBA{\cdot}PF_6$, respectively. Subsequent X-ray crystallographic analysis of the 1:3 complex formed between TPP51C15 and $DBA{\cdot}PF_6$ revealed (Figure 1.39) the formation of a *triple-stranded* [4]pseudorotaxane, in which each DBA^+ cation nestles into one of the three polyether loops present in the crown ether's framework. Stabilization of this four-component supermolecule arises as a consequence of both N^+–H···O and C–H···O hydrogen bonding interactions. Upon closer investigation, it was discovered that, yet again, the PF_6^- anion plays a prominent role in the solid-state superstructure. One of the three PF_6^- anions is located almost centrally within a cleft present in the $[TPP51C15{\cdot}(DBA)_3]^{3+}$ supermolecule. This anion can be considered to be 'complexed' by the [4]pseudorotaxane *via* a series of C–H···F hydrogen bonding interactions to hydrogen atoms of (i) the hydroquinone rings of the crown ether, and (ii) the benzylic methylene groups of the threaded DBA^+ cations.

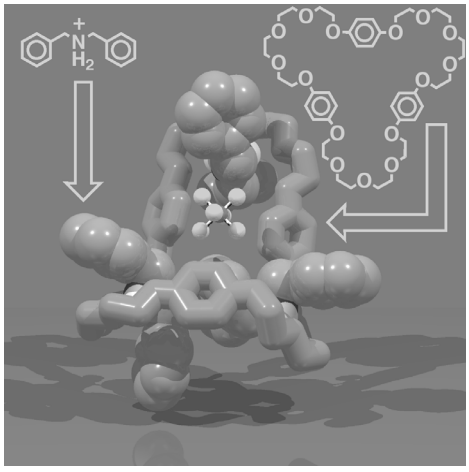

Figure 1.39. The extended crown ether TPP51C15 co-crystallizes with *three* equivalents of $DBA{\cdot}PF_6$ to give a *triple-threaded* [4]pseudorotaxane $[TPP51C15{\cdot}(DBA)_3]^{3+}$. Note how a PF_6^- anion occupies a cleft in the superstructure.

By analogy with this triple-threaded superstructure, the X-ray crystallographic analysis of the 1:4 complex formed between TPP68C20 and $DBA{\cdot}PF_6$ revealed (Figure 1.40) the formation of a *quadruple-stranded* [5]pseudorotaxane. Once again, each DBA^+ cation

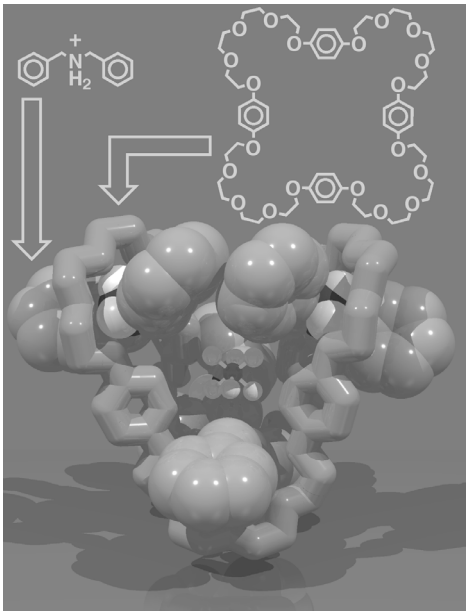

Figure 1.40. The extended crown ether TPP68C20 co-crystallizes with *four* equivalents of DBA·PF_6 to give a *quadruple-threaded* [5]pseudorotaxane $[TPP68C20\cdot(DBA)_4]^{4+}$. One PF_6^- anion is encapsulated completely within the superstructure.

resides in one of the four isolated polyether loops present in the crown ether's framework, and likewise, stabilization of this five-component supermolecule arises as a consequence of the familiar combination of both N^+–H···O and C–H···O hydrogen bonding interactions. A striking feature of this superstructure is once again associated with the positioning of one of the PF_6^- anions. In contrast with the [4]pseudo-rotaxane $[TPP51C15\cdot(DBA)_3]^{3+}$, the super-molecule generated using the larger TPP68C20 macrocycle has enough room in its interior to encapsulate[60] completely one of the PF_6^- anions. The complexation of this highly ordered PF_6^- anion is presumably stabilized by an array of C–H···F hydrogen bonding[50] interactions, as well as by a coulombic term arising from siting an anion within the influence of four, tetrahedrally disposed, NH_2^+ centers. Although the PF_6^- anions may not be influencing directly the formation of these four- and five-component supermolecules, respectively, the active role they play in contributing to the overall superstructure may be important nonetheless.

1.9. Conclusions

It has been possible, during much less than a decade, to assemble a molecular meccano kit, based on some well-known recognition motifs, that relies primarily upon the ability of

neutral macrocyclic polyethers—with [24]crown-8 constitutions and larger—to thread onto chains containing, for the most part, benzylic functions and secondary dialkylammonium centers. With the help of other edge-to-edge (*e.g.*, the carboxylic acid hydrogen-bonded dimer) and face-to-face (*e.g.*, π–π stacking of aromatic ring systems) interactions, supermolecules and supramolecular arrays can be formed that, in some instances, exist both in solution and the solid state – and in other instances exist only in solution. There are also a few cases where the supramolecular architectures differ in the solid and solution states. The recognition of hexafluorophosphate anions by the positively charged supermolecules appears to be one factor that can appreciably influence the adoption of a particular supramolecular architecture in the solid state that is not necessarily seen at all in the solution state.

1.10. References and Notes

1. (a) Nicolaou, K. C.; Vourloumis, D.; Winssinger, N.; Baran, P. S.; *Angew. Chem., Int. Ed.* **2000**, *39*, 44–122. (b) Sierra, M. A.; de la Torre, M. C.; *Angew. Chem., Int. Ed.* **2000**, *39*, 1538–1559.
2. Nicolaou, K. C.; Sorensen, E. J. *Classics in Total Synthesis*; Wiley-VCH: Weinheim, 1996.
3. Woodward, R. B.; Cava, M. P.; Ollis, W. D.; Hunger, A.; Daeniker, H. U.; Schenker, K. *J. Am. Chem. Soc.* **1954**, *76*, 4749–4751.
4. Corey, E. J.; Weinshenker, N. M.; Schaaf T. K.; Huber, W. *J. Am. Chem. Soc.* **1969**, *91*, 5675–5677.
5. Suh E. M.; Kishi, Y. *J. Am. Chem. Soc.* **1994**, *116*, 11205–11206.
6. (a) Nicolaou, K. C.; Yang, Z.; Liu, J. J.; Ueno, H.; Nantermet, P. G.; Guy, R. K.; Claiborne, C. F.; Renaud, J.; Couladouros, E. A.; Paulvannan K.; Sorensen, E. J. *Nature (London)* **1994**, *367*, 630–634. (b) Holton, R. A.; Somoza, C.; Kim, H.-B.; Liang, F.; Beidiger, R. J.; Boatman, P. D.; Shindo, M.; Smith, C. C.; Kim, S. C.; Nadizadeh, H.; Suzuki, Y.; Tao, C. L.; Vu, P.; Tang, S. H.; Zhang, P. S.; Murthi, K. K.; Gentile L. N.; Liu, J. H. *J. Am. Chem. Soc.* **1994**, *116*, 1597–1598. (c) Holton, R. A.; Kim, H.-B.; Somoza, C.; Liang, F.; Biediger, R. J.; Boatman, P. D.; Shindo, M.; Smith, C. C.; Kim, S. C.; Nadizadeh, H.; Suzuki, Y.; Tao, C. L.; Vu, P.; Tang,

S. H.; Zhang, P. S.; Murthi, K. K.; Gentile L. N.; Liu, J. H. *J. Am. Chem. Soc.* **1994**, *116*, 1599–1600. (d) Masters, J. J.; Link, J. T.; Snyder, L. B.; Young, W. B.; Danishefsky, S. J. *Angew. Chem., Int. Ed. Engl.* **1995**, *34*, 1723–1726.

7. (a) Nicolaou, K. C.; Theodorakis, E. A.; Rutjes, F. P. T. J.; Tiebes, J.; Sato, M.; Unterseller, E.; Xiao, X.-Y. *J. Am. Chem. Soc.* **1995**, *117*, 1173–1174. (b) Nicolaou, K. C.; Rutjes, F. P. J. T.; Theodorakis, E. A.; Tiebes, J.; Sato, M.; Untersteller, E. *J. Am. Chem. Soc.* **1995**, *117*, 10252–10263.

8. Natural products are not the sole targets in the realm of covalent synthesis. Indeed, the potential for generating large monodisperse targets—utilizing the chemistry of the covalent bond—is perhaps best demonstrated in the dendrimer field. For examples, see: (a) Ardoin, N.; Astruc, D. *Bull. Chim. Soc. Fr.* **1995**, *132*, 875–909. (b) Dvornic, P. R.; Tomalia, D. A. *Curr. Opin. Colloid Interface Sci.* **1996**, *1*, 221–235. (c) Newkome, G. R.; Moorefield, C. N.; Vögtle, F. *Dendritic Molecules: Concepts, Syntheses, Perspectives*; VCH: Weinheim, 1996. (d) Moore, J. S. *Acc. Chem. Res.* **1997**, *30*, 402–413. (e) Matthews, O. A.; Shipway, A. N.; Stoddart, J. F. *Prog. Polym. Sci.* **1998**, *23*, 1–56. (f) Balzani, V.; Campagna, S.; Denti, G.; Juris, A.; Serroni, S.; Venturi, M. *Acc. Chem. Res.* **1998**, *31*, 26–34. (g) Emrick, T.; Fréchet, J. M. J. *Curr. Opin. Colloid Interface Sci.* **1999**, *4*, 15–23. (h) Kim, Y.; Zeng, F. W.; Zimmerman, S. C. *Chem. Eur. J.* **1999**, *5*, 2133–2138. (i) Newkome, G. R.; Childs, B. J.; Rourk, M. J.; Baker, G. R.; Moorefield, C. N. *Biotech. Bioeng.* **1999**, *61*, 243–253. (j) Newkome, G. R.; He, E. F.; Moorefield, C. N. *Chem. Rev.* **1999**, *99*, 1689–1746. (k) Bosman, A. W.; Janssen, H. M.; Meijer, E. W. *Chem. Rev.* **1999**, *99*, 1665–1688. (l) Fischer, M.; Vögtle, F. *Angew. Chem., Int. Ed*. **1999**, *38*, 885–905. A combination of both *molecular* and *supramolecular* synthesis has been employed in the construction of large dendritic superstructures, see: (m) Prokhorova, S. A.; Sheiko, S. S.; Ahn, C. H.; Percec, V.; Moller, M. *Macromolecules* **1999**, *32*, 2653–2660. (n) Percec, V.; Ahn, C. H.; Bera, T. K.; Ungar, G.; Yeardley, D. J. P. *Chem. Eur. J.* **1999**, *5*, 1070–1083. (o) Yeardley, D. J. P.; Ungar, G.; Percec, V.; Holerca, M. N.; Johansson, G. *J. Am. Chem. Soc.* **2000**, *122*, 1684–1689. (p) Percec, V.; Cho, W.-D.; Ungar, G. *J. Am. Chem. Soc.* **2000**, *122*, 10273–10281.

9. (a) Mascal, M. *Contemp. Org. Synth.* **1994**, *1*, 31–46. (b) Lehn, J.-M. *Supramolecular Chemistry*; VCH: Weinheim, 1995. (c) *Comprehensive Supramolecular Chemistry*; Atwood, J. L.; Davies, J. E. D.; MacNicol, D. D.; Vögtle, F., Eds.; Pergamon: Oxford, 1996; 11 vols. (d) Schneider H.-J.; Yatsimirsky, A. *Principles and Methods in Supramolecular Chemistry*; Wiley: Chichester, 2000.

10. Fyfe, M. C. T.; Stoddart, J. F. *Acc. Chem. Res.* **1997**, *30*, 393–401.

11. (a) Seto, C. T.; Whitesides, G. M. *J. Am. Chem. Soc.* **1993**, *115*, 1330–1340. (b) Kotera, M.; Lehn, J.-M.; Vigneron, J.-P. *J. Chem. Soc., Chem. Commun*. **1994**, 197–199. (c) Subramanian, S.; Zaworotko, M. J. *Coord. Chem. Rev.* **1994**, *137*, 357–401. (d) Leigh, D. A.; Murphy, A.; Smart, J. P.; Slawin, A. M. Z. *Angew. Chem., Int. Ed. Engl*. **1997**, *36*, 728–732. (e) Jeffrey, G. A. *An Introduction to Hydrogen Bonding*; Oxford University Press: New York, 1997. (f) Philp, D.; Robinson, J. M. A. *J. Chem. Soc., Perkin Trans. 2* **1998**, 1643–1650. (g) Martin, T.; Obst, U.;

Rebek, J., Jr. *Science* **1998**, *281*, 1842–1845. (h) Melendez, R. E.; Hamilton, A. D. *Top. Curr. Chem.* **1998**, *198*, 97–129. (i) Sijbesma, R. P.; Meijer, E. W. *Curr. Opin. Colloid Interface Sci.* **1999**, *4*, 24–32. (j) Seel, C.; Parham, A. H.; Safarowsky, O.; Hübner, G. M.; Vögtle, F. *J. Org. Chem.* **1999**, *64*, 7236–7242.

12. (a) Sauvage, J.-P. *Acc. Chem. Res.* **1998**, *31*, 611–619. (b) Fujita, M. *Chem. Soc. Rev.* **1998**, *27*, 417–425. (c) Saalfrank, R. W.; Bernt, I. *Curr. Opin. Solid State Mater. Sci.* **1998**, *3*, 407–413. (d) Raymo, F. M.; Stoddart, J. F. *Curr. Opin. Colloid Interface Sci.* **1998**, *3*, 150–159. (e) Batten, S. R.; Robson, R. *Angew. Chem., Int. Ed.* **1998**, *37*, 1461–1494. (f) Fujita, M. *Acc. Chem. Res.* **1999**, *32*, 53–61. (g) Caulder, D. L.; Raymond, K. N. *J. Chem. Soc., Dalton Trans.* **1999**, 1185–1200. (h) Constable, E. C.; Haverson, P. *Polyhedron* **1999**, *18*, 3093–3106. (i) Caulder, D. L.; Raymond, K. N. *Acc. Chem. Res.* **1999**, *32*, 975–982. (j) Leininger, S.; Olenyuk, B.; Stang, P. J. *Chem. Rev.* **2000**, *100*, 853–907.

13. (a) Rebek, J., Jr.; Nemeth, D. *J. Am. Chem. Soc.* **1986**, *108*, 5637–5638. (b) Burley, S. K.; Petsko, G. A. *J. Am. Chem. Soc.* **1986**, *108*, 7995–8001. (c) Hamilton, A. D.; Van Engen, D. *J. Am. Chem. Soc.* **1987**, *109*, 5035–5036. (d) Zimmerman, S. C.; Vanzyl, C. M. *J. Am. Chem. Soc.* **1987**, *109*, 7894–7896. (e) Hunter, C. A.; Sanders, J. K. M. *J. Am. Chem. Soc.* **1990**, *112*, 5525–5534. (f) Cozzi, F.; Cinquini, M.; Annunziata, R.; Dwyer, T.; Siegel, J. S. *J. Am. Chem. Soc.* **1992**, *114*, 5729–5733. (g) Hunter, C. A. *Angew. Chem., Int. Ed. Engl.* **1993**, *32*, 1584–1586. (h) Hunter, C. A. *Chem. Soc. Rev.* **1994**, *23*, 101–109. (i) Claessens, C. G.; Stoddart, J. F. *J. Phys. Org. Chem.* **1997**, *10*, 254–272. (j) Nelson, J. C.; Saven, J. G.; Moore, J. S.; Wolynes, P. G. *Science* **1997**, *277*, 1793–1796. (k) Lokey, R. S.; Kwok, Y.; Guelev, V.; Pursell, C. J.; Hurley, L. H.; Iverson, B. L. *J. Am. Chem. Soc.* **1997**, *119*, 7202–7210. (l) Whitten, D. G.; Chen, L. H.; Geiger, H. C.; Perlstein, J.; Song, X. D. *J. Phys. Chem. B* **1998**, *102*, 10098–10111.

14. An edge-to-face interaction between two aromatic rings is simply an example of a C–H···π interaction. In general terms, the C–H donor does not necessarily have to be part of an aromatic ring. For literature on the C–H···π interaction, see: (a) Ferguson, S. B.; Diederich, F. *Angew. Chem., Int. Ed. Engl.* **1986**, *25*, 1127–1129. (b) Nishio, M.; Hirota, M. *Tetrahedron* **1989**, *45*, 7201–7245. (c) Oki, M. *Acc. Chem. Res.* **1990**, *23*, 351–356. (d) Etter, M. C. *J. Phys. Chem.* **1991**, *95*, 4601–4610. (e) Zaworotko, M. J. *Chem. Soc. Rev.* **1994**, *23*, 283–288. (f) Boyd, D. R.; Evans, T. A.; Jennings, W. B.; Malone, J. F.; O'Sullivan, W.; Smith, A. *Chem. Commun.* **1996**, 2269–2270. (g) Ashton, P. R.; Hörner, B.; Kocian, O.; Menzer, S.; White, A. J. P.; Stoddart, J. F.; Williams, D. J. *Synthesis* **1996**, 930–940. (h) Adams, H.; Carver, F. J.; Hunter, C. A.; Morales, J. C.; Seward, E. M. *Angew. Chem., Int. Ed. Engl.* **1996**, *35*, 1542–1544. (i) Carver, F. J.; Hunter, C. A.; Seward, E. M. *Chem. Commun.* **1998**, 775–776. (j) Desiraju, G. R.; Steiner, T. *The Weak Hydrogen Bond in Structural Chemistry and Biology*; Oxford University Press: Oxford, 1999.

15. (a) Ben-Naim, A. *Hydrophobic Interactions*; Plenum Press: New York & London, 1980. (b) Tanford, C. *The Hydrophobic Effect: Formation of Micelles and Biological Membranes*; Wiley:

Chichester, 2nd Edn., 1980. (c) Privalov, P. L.; Gill, S. J. *Pure Appl. Chem.* **1989**, *61*, 1097–1104. (d) Blokzijl, W.; Engberts, J. B. F. N. *Angew. Chem., Int. Ed. Engl.* **1993**, *32*, 1545–1579. (e) Silverstein, K. A. T.; Hayment, A. D. J.; Dill, K. A. *J. Am. Chem. Soc.* **1998**, *120*, 3166–3175. (f) Rekharsky, M. V.; Inoue, Y. *Chem. Rev.* **1998**, *98*, 1875–1917. (g) Marmur, A. *J. Am. Chem. Soc.* **2000**, *122*, 2120–2121.

16. (a) Msayib, K. J.; Watt, C. I. F. *Chem. Soc. Rev.* **1992**, *21*, 237–243. (b) Aida, M. *J. Mol. Struct.* **1994**, *117*, 45–53. (c) Hamelin, B.; Jullien, L.; Derouet, C.; du Penhoat, C. H.; Berthault, P. *J. Am. Chem. Soc.* **1998**, *120*, 8438-8447. (d) Mascal, M.; Hansen, J.; Fallon, P. S.; Blake, A. J.; Heywood, B. R.; Moore, M. H.; Turkenburg, J. P. *Chem. Eur. J.* **1999**, *5*, 381–384. (e) du Mont, W. W.; Ruthe, F. *Coord. Chem. Rev.* **1999**, *189*, 101–133. (f) Müller-Dethlefs, K.; Hobza, P. *Chem. Rev.* **2000**, *100*, 143–167. (g) Sheinerman, F. B.; Norel, R.; Honig, B. *Curr. Opin. Struct. Biol.* **2000**, *10*, 153–159.
17. (a) Nevinskii, G. A. *Mol. Biol.* **1995**, *29*, 6–19. (b) Ohta, K.; Ikejima, M.; Moriya, M.; Hasebe, H.; Yamamoto, I. *J. Mater. Chem.* **1998**, *8*, 1971–1977. (c) Novoa, J. J.; Lafuente, P.; Mota, F. *Chem. Phys. Lett.* **1998**, *290*, 519–525. (d) Street, A. G.; Mayo, S. L. *Proc. Natl. Acad. Sci. USA* **1999**, *96*, 9074–9076. (e) Nakamura, K.; Houk, K. N. *Org. Lett.* **1999**, *1*, 2049–2051. (f) Issaenko, S. A.; Harris, A. B. *Phys. Rev. E* **2000**, *61*, 2777–2791. (g) Berezovsky, I. N.; Esipova, N. G.; Tumanyan, V. G.; Namiot, V. A. *J. Bio. Molec. Struct. Dyn.* **2000**, *17*, 799–809.
18. (a) Lindsey, J. S. *New J. Chem.* **1991**, *15*, 153–180. (b) Philp, D.; Stoddart, J. F. *Synlett* **1991**, 445–458. (c) Whitesides, G. M.; Mathias, J. P.; Seto, C. T. *Science* **1991**, *154*, 1312–1319. (d) Lawrence, D. S.; Jiang, T.; Levett, M. *Chem. Rev.* **1995**, *95*, 2229–2260. (e) Philp, D.; Stoddart, J. F. *Angew. Chem. Int., Ed. Engl.* **1996**, *35*, 1154–1196. (f) Stang, P. J.; Olenyuk, B. *Acc. Chem. Res.* **1997**, *30*, 502–518. (g) Cusack, L.; Rao, S. N.; Wenger, J.; Fitzmaurice, D. *Chem. Mater.* **1997**, *9*, 624–631. (h) Conn, M. M.; Rebek, J., Jr. *Chem. Rev.* **1997**, *97*, 1647–1668. (i) Linton, B.; Hamilton, A. D. *Chem. Rev.* **1997**, *97*, 1669–1680. (j) Breen, T. L.; Tien, J.; Oliver, S. R. J.; Hadzic, T.; Whitesides, G. M. *Science* **1999**, *284*, 948–951. (k) Tomalia, D. A.; Wang Z. G.; Tirrel, M. *Curr. Opin. Colloid Interface Sci.* **1999**, *4*, 3–5.
19. Fyfe, M. C. T.; Stoddart, J. F. *Coord. Chem. Rev.* **1999**, *183*, 139–155.
20. (a) Schill, G. *Catenanes, Rotaxanes, and Knots*; Academic Press: New York, 1971. (b) Breault, G. A.; Hunter, C. A.; Mayers, P. C. *Tetrahedron* **1999**, *55*, 5265–5293. (c) *Molecular Catenanes, Rotaxanes and Knots*; Sauvage, J.-P.; Dietrich-Buchecker, C., Eds.; Wiley-VCH: Weinhem, 1999. (d) Hubin, T. J.; Kolchinski, A. G.; Vance, A. L.; Busch, D. H. *Adv. Supramol. Chem.* **1999**, *5*, 237–357.
21. Amabilino, D. B.; Stoddart, J. F. *Chem. Rev.* **1995**, *95*, 2725–2828.
22. (a) *Crystal Engineering. The Design of Organic Solids*; Desiraju, G. R., Ed.; Elsevier: Amsterdam, 1989. (b) Desiraju, G. R. *Angew. Chem., Int. Ed. Engl.* **1995**, *34*, 2311–2327. (c) *The Crystal as a Supramolecular Entity*; Desiraju, G. R., Ed.; Wiley: Chichester, 1996. (d) Desiraju, G. R. *Chem.*

Commun. **1997**, 1475–1482. (e) Desiraju, G. R. *Curr. Opin. Solid State Mater. Sci.* **1997**, *2*, 451–454. (f) Nangia, A.; Desiraju, G. R. *Top. Curr. Chem.* **1998**, *198*, 57–95.

23. (a) Fyfe, M. C. T.; Stoddart, J. F.; Williams, D. J. *Struct. Chem.* **1999**, *10*, 243–259. (b) Fyfe, M. C. T.; Stoddart, J. F. *Adv. Supramol. Chem*. **1999**, *5*, 1–53.
24. (a) Pedersen, C. J. *J. Am. Chem. Soc.* **1967**, *89*, 7017–7036. (b) Cram, D. J.; Cram, J. M. *Science* **1974**, *183*, 803–809. (c) Cram, D. J.; Cram, J. M. *Acc. Chem. Res.* **1978**, *11*, 8–14. (d) De Jong, F.; Reinhoudt, D. N. *Adv. Phys. Org. Chem.* **1980**, *17*, 279–433. (e) Cram, D. J.; Trueblood, K. N. *Top. Curr. Chem.* **1981**, *98*, 43–106. (f) Sutherland, I. O. *Chem. Soc. Rev.* **1986**, *15*, 63–91. (g) Stoddart, J. F. *Top. Stereochem.* **1987**, *17*, 205–288. (h) Izatt, R. M.; Wang, T.; Hathaway, J. K.; Zhang, X. X.; Curtis, J. C.; Bradshaw, J. S.; Zhu, C. Y.; Huszthy, P. *J. Incl. Phenom.* **1994**, *17*, 157–175.
25. (a) Montalti, M.; Prodi, L. *Chem. Commun.* **1998**, 1461–1462. (b) Yamaguchi, N.; Hamilton, L. M.; Gibson, H. W. *Angew. Chem., Int. Ed.* **1998**, *37*, 3275–3279. (c) Ishow, E.; Credi, A.; Balzani, V.; Spadola, F.; Mandolini, L. *Chem. Eur. J.* **1999**, *5*, 984–989. (d) Bryant, W. S.; Guzei, I. A.; Rheingold, A. L.; Merola, J. S.; Gibson, H. W. *J. Org. Chem.* **1998**, *63*, 7634–7639. (e) Bryant, W. S.; Guzei, I. A.; Rheingold, A. L.; Gibson, H. W. *Org. Lett.* **1999**, *1*, 47–50. (f) Yamaguchi, N.; Gibson, H. W. *Chem. Commun.* **1999**, 789–790. (g) Meillon, J. C.; Voyer, N.; Biron, E.; Sanschagrin, F.; Stoddart, J. F. *Angew. Chem., Int. Ed.* **2000**, *39*, 143–145.
26. (a) Kolchinski, A. G.; Alcock, N. W.; Roesner, A.; Busch, D. H. *Chem. Commun.* **1998**, 1437–1438. (b) Takata, T.; Kawasaki, H.; Asai, S.; Kihara, N.; Furusho, Y. *Chem. Lett.* **1999**, 111–112. (c) Takata, T.; Kawasaki, H.; Asai, S.; Furusho, Y.; Kihara, N. *Chem. Lett.* **1999**, 223–224. (d) Kawasaki, H.; Kihara, N.; Takata, T. *Chem. Lett.* **1999**, 1015–1016. (e) Furusho, Y.; Hasegawa, T.; Tsuboi, A.; Kihara, N.; Takata, T. *Chem. Lett.* **2000**, 18–19. (f) Rowan, S. J.; Cantrill, S. J.; Stoddart, J. F.; White, A. J. P.; Williams, D. J. *Org. Lett.* **2000**, *2*, 759–762.
27. Ashton, P. R.; Campbell, P. J.; Chrystal, E. J. T.; Glink, P. T.; Menzer, S.; Philp, D.; Spencer, N.; Stoddart, J. F.; Tasker, P. A.; Williams, D. J. *Angew. Chem., Int. Ed. Engl.* **1995**, *34*, 1865–1869.
28. Crown ethers with less than 24 atoms in their macrorings have been observed to form *face-to-face* complexes with secondary dialkylammonium ions. See: (a) Metcalfe, J. C.; Stoddart, J. F.; Jones, G. *J. Am. Chem. Soc.* **1977**, *99*, 8317–8319. (b) Krane, J.; Aune, O. *Acta Chem. Scand.* **1980**, *34B*, 397–401. (c) Metcalfe, J. C.; Stoddart, J. F.; Jones, G.; Atkinson, A.; Kerr, I. S.; Williams, D. J. *J. Chem. Soc., Chem. Commun.* **1980**, 540–543. (d) Abed-Ali, S. S.; Brisdon, B. J.; England, R. *J. Chem. Soc., Chem. Commun.* **1987**, 1565–1566.
29. Kolchinski, A. G.; Busch, D. H.; Alcock, N. W. *J. Chem. Soc., Chem. Commun.* **1995**, 1289–1291.
30. Ashton, P. R.; Chrystal, E. J. T.; Glink, P. T.; Menzer, S.; Schiavo, C.; Spencer, N.; Stoddart, J. F.; Tasker, P. A.; White, A. J. P.; Williams, D. J. *Chem. Eur. J.* **1996**, *2*, 709–728.
31. Gutmann, V. *Coord. Chem. Rev.* **1976**, *18*, 225–255.

32. Ashton, P. R.; Campbell, P. J.; Chrystal, E. J. T.; Glink, P. T.; Menzer, S.; Schiavo, C.; Stoddart, J. F.; Tasker, P. A.; Williams, D. J. *Angew Chem., Int. Ed. Engl.* **1995**, *34*, 1869–1871.

33. Ashton, P. R.; Fyfe, M. C. T.; Glink, P. T.; Menzer, S.; Stoddart, J. F.; White, A. J. P.; Williams, D. J. *J. Am. Chem. Soc.* **1997**, *119*, 12514–12524.

34. (a) Leiserowitz, L. *Acta Crystallogr.* **1976**, *B32*, 775–802. (b) Berkovitch-Yellin, Z.; Leiserowitz, L. *J. Am. Chem. Soc.* **1982**, *104*, 4052–4064. (c) Kolotuchin, S. V.; Fenlon, E. E.; Wilson, S. R.; Loweth, C. J.; Zimmerman, S. C. *Angew. Chem., Int. Ed. Engl.* **1995**, *34*, 2654–2657. (d) Aakeröy, C. B. *Acta Crystallogr.* **1997**, *B53*, 569–586. (e) Kolotuchin, S. V.; Thiessen, P. A.; Fenlon, E. E.; Wilson, S. R.; Loweth, C. J.; Zimmerman, S. C. *Chem. Eur. J.* **1999**, *5*, 2537–2547.

35. Bailey, M.; Brown, C. J. *Acta Crystallogr.* **1967**, *22*, 387–391.

36. Alcala, R.; Martinez-Carrera, S. *Acta Crystallogr.* **1972**, *B28*, 1671–1677.

37. (a) Yang, J.; Marendaz, J. L.; Geib, S. J.; Hamilton, A. D. *Tetrahedron Lett.* **1994**, *35*, 3665–3668. (b) Valiyaveettil, S.; Enkelmann, V.; Moessner, K.; Müllen, K. *Macromol. Symp.* **1996**, *102*, 165–173. (c) Zimmerman, S. C.; Zeng, F.; Reichert, D. E. C.; Kolotuchin, S. V. *Science* **1996**, *271*, 1095–1098.

38. (a) Ashton, P. R.; Collins, A. N.; Fyfe, M. C. T.; Menzer, S.; Stoddart, J. F.; Williams, D. J. *Angew. Chem., Int. Ed. Engl.* **1997**, *36*, 735–739. (b) Fyfe, M. C. T.; Stoddart, J. F.; Collins, A. N.; Williams, D. J. in *Molecular Recognition and Inclusion, Lyon 1996*, Coleman, A. W., Ed.; Kluwer: Netherlands, 1998, pp. 333-336. (c) Ashton, P. R.; Fyfe, M. C. T.; Hickingbottom, S. K.; Menzer, S.; Stoddart, J. F.; White, A. J. P.; Williams, D. J. *Chem. Eur. J.* **1998**, *4*, 577–589.

39. For other examples of daisy chain-like superstructures, see: (a) Hirotsu, K.; Higuchi, T.; Fujita, K.; Ueda, T.; Shinoda, A.; Imoto, T.; Tabushi, I. *J. Org. Chem.* **1982**, *47*, 1143–1144. (b) Zanotti-Gerosa, A.; Solari, E.; Giannini, L.; Chiesi-Villa. A.; Rizzoli, C. *Chem. Commun.* **1996**, 119–120. (c) Mentzafos, D.; Terzis, A.; Coleman, A. W.; de Rango, C. *Carbohydr. Res.* **1996**, *282*, 125–135. (d) Ashton, P. R.; Parsons, I. W.; Raymo, F. M.; Stoddart, J. F.; White, A. J. P.; Williams, D. J.; Wolf, R. *Angew. Chem., Int. Ed.* **1998**, *37*, 1913–1916. (e) Yamaguchi, N.; Nagvekar, D. S.; Gibson, H. W. *Angew. Chem., Int. Ed.* **1998**, *37*, 2361–2364. (f) Mirzoian, A.; Kaifer, A. E. *Chem. Commun.* **1999**, 1603–1604. (g) Bülger, J.; Sommerdijk, N. A. J. M.; Visser, A. J. W. G.; van Hoek, A.; Nolte, R. J. M.; Engbersen, J. F. J.; Reinhoudt, D. N. *J. Am. Chem. Soc.* **1999**, *121*, 28–33.

40. (a) Ashton, P. R.; Baxter, I.; Cantrill, S. J.; Fyfe, M. C. T.; Glink, P. T.; Stoddart, J. F.; White, A. J. P.; Williams, D. J. *Angew. Chem., Int. Ed.* **1998**, *37*, 1294–1297.

41. For a discussion of (pseudo)polyrotaxane topologies, see: (a) Amabilino, D. B.; Parsons, I. W.; Stoddart, J. F. *Trends Polym. Sci.* **1994**, *2*, 146–152. (b) Gibson, H. W.; Bheda, M. C.; Engen, P. T. *Prog. Polym. Sci.* **1994**, *19*, 843–945. For other examples of (pseudo)polyrotaxanes, see: (c) Herrmann, W.; Schneider, M.; Wenz, G. *Angew. Chem., Int. Ed. Engl.* **1997**, *36*, 2511–2515. (d) Gong, C. G.; Gibson, H. W. *Angew. Chem., Int. Ed.* **1998**, *37*, 310–314. (e) Harada, A. *Acta*

Polym. **1998**, *49*, 3–17. (f) Park, K. M.; Heo, J.; Roh, S. G.; Jeon, Y. M.; Whang, D.; Kim, K. *Mol. Cryst. Liq. Cryst. A* **1999**, *327*, 65–70. (g) Raymo, F. M.; Stoddart, J. F. *Chem. Rev.* **1999**, *99*, 1643–1663.

42. (a) Ashton, P. R.; Glink, P. T.; Stoddart, J. F.; Menzer, S.; Tasker, P. A.; White, A. J. P.; Williams, D. J. *Tetrahedron Lett.* **1996**, *37*, 6217–6220. (b) Ashton, P. R.; Glink, P. T.; Stoddart, J. F.; Tasker, P. A.; White; A. J. P.; Williams, D. J. *Chem. Eur. J.* **1996**, *2*, 729–736. (c) Cantrill, S. J.; Fulton, D. A.; Fyfe, M. C. T.; Stoddart, J. F.; White A. J. P.; Williams, D. J. *Tetrahedron Lett.* **1999**, *40*, 3669–3672. (d) Cantrill, S. J.; Fyfe, M. C. T.; Heiss, A. M.; Stoddart, J. F.; White, A. J. P.; Williams, D. J. *Chem. Commun.* **1999**, 1251–1252. (e) Rowan, S. J.; Cantrill, S. J.; Stoddart, J. F. *Org. Lett.* **1999**, *1*, 129–132. (f) Cantrill, S. J.; Rowan, S. J.; Stoddart, J. F. *Org. Lett.* **1999**, *1*, 1363–1366.
43. (a) Rowan, S. J.; Stoddart, J. F. *J. Am. Chem. Soc.* **2000**, *122*, 164–165. (b) Cao, J.; Fyfe, M. C. T.; Stoddart, J. F.; Cousins, G. R. L.; Glink, P. T. *J. Org. Chem.* **2000**, *65*, 1937–1946.
44. Ashton, P. R.; Bartsch, R. A.; Cantrill, S. J.; Hanes, R. E., Jr.; Hickingbottom, S. K.; Lowe, J. N.; Preece, J. A.; Stoddart, J. F.; Talanov, V. S.; Wang, Z.-H. *Tetrahedron Lett.* **1999**, *40*, 3661–3664.
45. (a) Brown, G. R.; Foubister, A. J. *J. Med. Chem.* **1983**, *26*, 590–592. (b) Kavallieratos, K.; Sachleben, R. A.; Van Berkel, G. J.; Moyer, B. A. *Chem. Commun.* **2000**, 187–188. (c) Levitskaia, T. G.; Bryan, J. C.; Sachleben, R. A.; Lamb, J. D.; Moyer, B. A. *J. Am. Chem. Soc.* **2000**, *122*, 554–562. (d) Bryan, J. C.; Kavallieratos, K.; Sachleben, R. A. *Inorg. Chem.* **2000**, *39*, 1568–1572.
46. Cantrill, S. J.; Preece, J. A.; Stoddart, J. F.; Wang, Z.-H.; White, A. J. P.; Williams, D. J. *Tetrahedron* **2000**, *56*, 6675–6681.
47. Bryan, J. C.; Sachleben, R. A.; Hay, B. P. *Inorg. Chim. Acta* **1999**, *290*, 86–94.
48. Bryan, J. C.; Bunick, G. J.; Sachleben, R. A. *Acta Crystallogr*. **1999**, *C55*, 250–252.
49. Ashton, P. R.; Cantrill, S. J.; Preece, J. A.; Stoddart, J. F.; Wang, Z.-H.; White, A. J. P.; Williams, D. J. *Org. Lett.* **1999**, *1*, 1917–1920.
50. (a) Teff, D. J.; Huffman, J. C.; Caulton, K. G. *Inorg. Chem*. **1997**, *36*, 4372–4380. (b) Thalladi, V. R.; Weiss, H.-C.; Bläser, D.; Boese, R.; Nangia, A.; Desiraju, G. R. *J. Am. Chem. Soc*. **1998**, *120*, 8702–8710. (c) Steiner, T. *Acta Crystallogr*. **1998**, *B54*, 456–463. (d) Grepioni, F.; Cojazzi, G.; Draper, S. M.; Scully, N.; Braga, D. *Organometallics* **1998**, *17*, 296–307. (e) Dai, C.; Nguyen, P.; Marder, T. B.; Scott, A. J.; Clegg W.; Viney, C. *Chem. Commun*. **1999**, 2493–2494. (f) Renak, M. L.; Bartholomew, G. P.; Wang, S.; Ricatto, P. J.; Lachicotte, R. J.; Bazan, G. C. *J. Am. Chem. Soc*. **1999**, *121*, 7787–7799.
51. Cantrill, S. J.; Fulton, D. A.; Heiss, A. M.; Pease, A. R.; Stoddart, J. F.; White, A. J. P.; Williams, D. J. *Chem. Eur. J.* **2000**, *6*, 2274–2287.
52. Cantrill, S. J.; Fyfe, M. C. T.; Heiss, A. M.; Stoddart, J. F.; White, A. J. P.; Williams, D. J. *Org. Lett.* **2000**, *1*, 61–64.

53. Krämer, R.; Lehn, J.-M.; Marquis-Rigault, A. *Proc. Natl. Acad. Sci. USA* **1993**, *90*, 5394–5398.
54 Ashton, P. R.; Collins, A. N.; Fyfe, M. C. T.; Glink, P. T.; Menzer, S.; Stoddart, J. F.; Williams, D. J. *Angew. Chem., Int. Ed. Engl.* **1997**, *36*, 59–62.
55. Fieters, M. C.; Fyfe, M. C. T.; Martínez-Díaz, M.-V.; Menzer, S.; Nolte, R. J. M.; Stoddart, J. F.; van Kan, P. J. M.; Williams, D. J. *J. Am. Chem. Soc*. **1997**, *119*, 8119–8120.
56. For synthetic molecular analogues of the photosynthetic special pair, see: Zheng, G.; Shibata, M.; Dougherty, T. J.; Pandey, R. K. *J. Org. Chem.* **2000**, *65*, 543–557.
57. Diesenhofer, J.; Michael, H. *Science* **1989**, *245*, 1463–1473.
58. Fyfe, M. C. T.; Lowe, J. N.; Stoddart, J. F.; Williams, D. J. *Org. Lett.* **2000**, *2*, 1221–1224.
59. Fyfe, M. C. T.; Glink, P. T.; Menzer, S.; Stoddart, J. F.; White, A. J. P.; Williams, D. J. *Angew. Chem., Int. Ed. Engl.* **1997**, *36*, 2068–2070.
60. For another example of PF_6^- anion encapsulation, see: McMorran, D. A.; Steel, P. J. *Angew. Chem., Int. Ed.* **1998**, *37*, 3295–3297.